Influence of shell effects on the dynamics of deep inelastic heavy-ion collisions

G. G. Adamyan and A. K. Nasirov
Institute of Nuclear Physics, Tashkent

N. V. Antonenko and R. V. Jolos
Joint Institute for Nuclear Research, Dubna

Fiz. Elem. Chastits At. Yadra **25**, 1379–1443 (November–December 1994)

The main approaches to the description of dissipative processes in heavy-ion physics are reviewed. A microscopic model of the authors for the description of the dissipation of the kinetic energy of the relative motion and the distribution of the excitation energy between the products of deep inelastic heavy-ion collisions is formulated. The calculations make it possible to draw a conclusion that is confirmed experimentally—the excitation energy is distributed approximately equally between the interacting nuclei and may even be concentrated on the light partner. The proposed microscopic model is used to find the coefficients of the master equation that determines the evolution of the dinuclear system in the charge and mass spaces. The influence of the shell structure of the nuclei on the process of simultaneous transfer of protons and neutrons in deep inelastic heavy-ion collisions is investigated. It is shown that the process of establishment of N/Z equilibrium is monotonic. Good agreement with experimental data is obtained. The calculated cross sections for the production of isotopes of light elements agree with the Q_{gg} systematics. An original method is developed for microscopic calculation of the energy "driving" potential of the dinuclear system. The microscopic "driving" potential carries more information about the paths of evolution of the dinuclear system. A fairly simple method for calculating the single-particle matrix elements of nucleon transitions in the dinuclear system is proposed.

INTRODUCTION

In heavy-ion collisions, various nuclear reactions can take place. To a large degree, their mechanism depends on the kinetic energy of the bombarding nuclei. On the scale of the kinetic energies, one can identify several points near which the reaction mechanism changes. Proceeding along this scale in the direction of increasing kinetic energy, the first point that we reach is the barrier for the interaction of the nuclei. If the kinetic energy of the incident ion is less than this value, the interaction of the nuclei is purely Coulomb. If short-range nuclear forces are to act, the nuclei must approach each other to a sufficiently short separation. For this the interaction barrier must be overcome. The next distinguished point corresponds to a velocity of the bombarding nucleus equal to the Fermi velocity, i.e., the kinetic energy per nucleon of the incident ion is equal to the Fermi energy. In the interval between these two points, direct reactions, deep inelastic heavy-ion collisions, and complete-fusion reactions take place.

Deep inelastic heavy-ion collisions give a unique possibility to study the interaction dynamics of two complex nuclei, since they occupy an intermediate position between such very different processes as direct reactions and reactions with formation of a compound nucleus. As in direct reactions, in deep inelastic collisions there is still a strong coupling between the entrance and exit channels of the reaction. The dispersions of the mass and charge distributions of both the products of deep inelastic collisions and the fission fragments are very large. Thus, dynamical and statistical aspects are simultaneously and clearly manifested in deep inelastic heavy-ion collisions. Despite the extensive experimental material that has been accumulated and numerous theoretical studies, we are still far from the construction of a unified microscopic picture of heavy-ion reactions at low energies ($\leqslant$10 MeV/nucleon). The mechanism responsible for the intense dissipation of kinetic energy (~hundreds of mega-electron-volts) has not yet been determined unambiguously. Very interesting questions relate to the distribution of the excitation energy between the reaction products, the relationships between the different reaction channels, and the isotope yields of individual elements.

A special feature of deep inelastic collisions is that they lead to a fundamentally new phenomenon in nuclear physics—the formation of a dinuclear system.[1–6] During the entire formation and evolution of the dinuclear system there is continuous redistribution of nucleons, excitation energy, and angular momentum between the nuclei. An unstable formation like a dinuclear system "lives" for the order of a few 10^{-21} s and decays before it achieves complete statistical equilibrium with respect to all degrees of freedom. The establishment of equilibrium between the proton and neutron numbers[5–7] occurs practically instantaneously in light systems and is a monotonic continuous process in heavy systems.[8–10] Nucleons are exchanged slowly between the parts of the dinuclear system. As it evolves, a dinuclear system can in principle pass with some definite probability through any macroscopic configuration allowed by the conservation laws for the particle number, charge, and total energy. A dinuclear system decays either for static reasons (dominance of forces of repulsion between the interacting nuclei) or for dynamical reasons (coupling of modes of motion).

Experimental data on the widths of the charge (mass) distributions of the reaction products,[5,6] the dependence of the yields of nuclei on their nucleon composition,[11–15] and data on the yields of light particles in collisions that lead to the formation of compound nuclei[16,17] indicate that as dinuclear systems evolve individual features of the nuclei are preserved, and shell effects play an important part. For example, for very heavy $^{238}U+^{238}U$ nuclei[18] one observes an unexpectedly intense diffusion of the protons compared with the other symmetric $^{208}Pb+^{208}Pb$ system.[19] The dispersions of the mass distributions in the $^{154}Sm+^{154}Sm$ and $^{144}Sm+^{144}Sm$ reactions differ strongly, this being explained in Ref. 20 by the large neutron binding energy in the second case. The cross sections for production of compound nuclei in the $^{100}Mo+^{100}Mo$ and $^{110}Pb+^{110}Pb$ reactions differ by four orders of magnitude, although the masses of the interacting nuclei differ by only 10 units.[21,22] The $^{16}O+^{92}Mo$ and $^{52}Cr+^{56}Fe$ (Ref. 23) or $^{40}Ar+^{232}Th$ and $^{32}S+^{238}U$ (Ref. 14) reactions, which lead to the same compound nucleus, give entirely different charge distributions, indicating different paths of evolution of the dinuclear systems. In the $^{238}U+^{48}Ca$ reaction[8,9] a large mass dispersion with small change in the mean mass number of the light fragment is observed, but in the $^{238}U+^{40}Ca$ reaction this is not so. Estimates show[24] that for the synthesis of heavy elements it is better to use a neutron-rich incident nucleus. The experiments of Refs. 1 and 5 indicate manifestation of shell effects in the $^{40}Ar+^{nat}Ag$ and $^{40}Ar+^{197}Au$ reactions. The yield of nuclei in them rapidly decreases with decrease of the atomic number Z from 18 to 9, but then begins to increase with decreasing Z and reaches the largest value for α particles. In addition, an enhanced yield of nuclei with closed shells and subshells is observed: ^{16}O, ^{12}C, ^{15}N. The nuclide yields also reflect the parity of Z and N. The even isotopes have larger production cross sections. Analysis of the experimental results showed that allowance for shell effects makes it possible to reproduce qualitatively the tendency in the behavior of $d\sigma/dZ$. The Q_{gg} systematics[1,5] is the most pronounced feature in the cross sections of the exit channels.

In a number of experiments it was shown that in the reactions with $^{58}Ni+^{197}Au$ (Refs. 25 and 26) and ^{56}Fe, $^{74}Ge+^{165}Ho$ (Refs. 27–33) the energy of the internal excitation is distributed approximately equally between the products of the binary reactions, and in the reactions with $^{52}Cr+^{208}Pb$ (Ref. 34), $^{238}U+^{124}Sn$, ^{110}Pb (Ref. 35) a greater part of the excitation energy is actually concentrated in the light fragment at relatively large losses of the kinetic energy. In the case of interaction of two nuclei homogeneous with respect to their structure, the excitation energy would be distributed fairly rapidly between the fragments in proportion to their masses. The considered experimental data confirm the idea that the individuality of the interacting nuclei is preserved even for a relatively high excitation energy of the dinuclear system and indicate that shell effects play a fundamental role in the evolution of the dinuclear system. The study of the influence of shell effects is topical in connection with planned experiments with radioactive beams, which will significantly extend the possibilities for investigating the mechanism of nuclear reactions. The basis for an analysis of these effects must be a microscopic model. In our view, theoretical study of the dynamics of dinuclear systems will make it possible to consider within a single approach deep inelastic collisions, quasifission, and fusion.

The simultaneous manifestation of dynamical and statistical effects in heavy-ion interactions extends the field of investigation and makes the interpretation of the experimental data more difficult, since one must consider a larger number of degrees of freedom. Because the nuclei have an internal structure, which is very complicated at the considered excitation energies, it is necessary to seek simplifications by choosing the most probable path of the evolution in the configuration space of the reaction instead of considering all possible paths and by introducing macroscopic characteristics (particle flux, friction, shape, etc.). It is a fundamental problem to understand these at the microscopic level. The dynamical and statistical characteristics are manifested to different degrees at different stages of heavy-ion collisions. This makes it possible to model separately each stage of the collision, and this also simplifies the theoretical treatment.

In a systematic microscopic theory, the evolution of dinuclear systems is determined by the time-dependent Schrödinger equation for the many-particle wave function of the system or by the Liouville equation for the many-particle density matrix. It is not possible to solve these equations without making certain simplifying assumptions. Moreover, exact solution of the equations gives more information than can be verified experimentally, since it is mainly inclusive characteristics of the reaction products that are observed in an experiment. On the other hand, the successes of relatively simple phenomenological and semimicroscopic models[36–44] indicate that not all degrees of freedom have a significant effect on the dynamics of the system. In such models, one identifies as important only certain collective (macroscopic) degrees of freedom, which are chosen *a priori* on the basis of the requirements of the interpretation of the experimental material. The number of collective degrees of freedom taken into account explicitly can be reduced by using experimentally established differences of their relaxation times.

Thus, the task of a microscopic theory is to find an effective Hamiltonian of the collective motion and interaction with the internal degrees of freedom. The coupling between the macroscopic and internal degrees of freedom is a source of irreversible processes in dinuclear systems such as transfer of mass, charge, etc. The existing models differ in the internal excitations that they introduce explicitly or implicitly. They may be coherent and incoherent particle–hole excitations in each of the nuclei and transfers of nucleons or clusters from nucleus to nucleus.[45,46] Since heavy-ion collisions are characterized by both coherent and stochastic forms of motion of the nucleons, there is the dilemma of which of these two processes is dominant in a reaction. The microscopic models based on a statistical description of the internal system do not make it possible to estimate the relative importance of the coherent and incoherent processes in heavy-ion collisions. A natural way out of this difficulty is to take into account simultaneously the incoherent and coherent properties of heavy-ion collisions on a unified basis or to test

each of these mechanisms in the description of different aspects of heavy-ion collisions.

The first possibility is partly realized in the approach called dissipative diabatic dynamics (DDD).[47,48] This model is restricted solely by the form of the coherent motion of the nucleons—their diabatic motion in the changing two-center mean field. The process of excitation of the nuclei includes only particle–hole states whose diabatic levels cross during the motion of the nuclei. Because of the diabatic nature of the single-particle motion, the coupling between the collective and internal degrees of freedom is coherent and nonlinear, in contrast to linear response theory. In the dissipative limit, the friction in the DDD model is equivalent to single-body friction ("wall" formula,[49] "piston" model[50]) if the time of establishment of local equilibrium is taken to be equal to the time required for a nucleon to pass through the nucleus.

Despite the clarity of the physical picture in the DDD model, there are certain doubts concerning the validity of the concept. First, there are no accurate estimates of the validity of assuming diabaticity of the single-particle motion. Second, as is shown by calculations of inelastic processes in nuclear collisions,[51] appreciable energy dissipation is observed even before the first crossing of the single-particle levels near the Fermi surface. Moreover, these excitations smear the Fermi surface, and the Landau–Zenerovskiĭ nucleon hopping mechanism loses its importance (the probability is small).

Numerous experimental data show that the dynamics of deep inelastic collisions is to a large degree determined by the process of mass and charge transfer between the nuclei. Up to now, two approaches, which start from opposite assumptions, have been developed to describe the establishment of equilibrium with respect to the charge mode in dinuclear systems. In the first approach, the exchange of protons is described as a stochastic process without allowance for inertial effects ("overdamped" regime).[7,52] In the second approach, the charge asymmetry is regarded as a collective mode.[6,53–55] The model of Ref. 55 is based on the method of a generalized density matrix[56] developed for the case of collective motion with large amplitude.[57,58] This model describes the dispersions of the charge distributions of the fragments for fixed mass asymmetry. The equations of the random-phase approximation are used to describe the high-lying isoscalar and isovector collective states of the dinuclear system.

The possibility that the transfer of mass (charge) in deep inelastic heavy-ion collisions is a collective process has been considered by Greiner's group.[42,59,60] In their theory of fragmentation, the evolution of the system along the mass-asymmetry coordinate is determined by a time-dependent Schrödinger equation. Integrating this equation along the classical trajectory of the relative motion of the colliding nuclei, one can determine the change in the width of the mass (charge) distribution. Of course, because of the adiabatic treatment of the process, quantum fluctuations are ignored. However, it is known that in the case of a rapid breaking of the neck the motion with respect to the mass-asymmetry mode becomes strongly nonadiabatic. In this model, the potential energy of the dinuclear system is calculated in the framework of the liquid-drop model with allowance for shell corrections. At the same time, it is assumed that at each instant the system is at the minimum of the potential energy with respect to the parameters describing the neck and the deformation of the nuclei.

Among the various approaches, transport (stochastic) models are most widely used to describe deep inelastic heavy-ion collisions.[61–75] The exchange of mass and charge and the transfer of energy and angular momentum of the relative motion to the internal degrees of freedom can be successfully interpreted as a diffusion process. By its nature, the interaction of nuclei is a nonequilibrium statistical process—the dinuclear system is not only excited but also relaxes to complete statistical equilibrium. Transport equations differ fundamentally from the Schrödinger equation. They describe the irreversible evolution of a probability distribution, and not an amplitude. All transport theories proceed from a division of the degrees of freedom of the system into a slow macroscopic degree and a rapidly relaxing internal degree; this leads to the neglect of coherence effects and correlations. By adopting explicitly or implicitly statistical hypotheses for the interaction operator of the collective and internal degrees of freedom, it is possible to deduce kinetic equations from the Liouville dynamical equation of motion. Such a derivation makes it possible to obtain microscopic transport coefficients. It is interesting to compare the transport coefficients obtained in the various models.[76,77] In the macroscopic diffusion models, the transport coefficients are assumed to be proportional to the ratio of the phase spaces of the states of the excited system, i.e., the direction of nucleon transfer is determined by the balance between the total energies of the different configurations of the dinuclear system. Some shell effects associated with the dependence of the binding energy on A and Z can be included in the potential energy ("driving" potential) of the dinuclear system by using experimental values of the binding energies of the nuclei of the dinuclear system. However, the neglect of the nucleon shell structure of the nuclei makes it impossible to interpret some experimental data. For example, the diffusion models that use a potential-energy surface cannot explain the strong growth in the dispersion of the mass distribution corresponding to a weak change in the mean masses of the reaction partners.[10,78]

In the microscopic approach, various authors developed transport models such as the random-matrix approximation (Refs. 61, 67, 71, and 75), the model of single-body dissipation,[68,69,72] and the linear-response model (Refs. 65, 66, 73, and 74), which stimulated the development of the theory of large-amplitude collective nuclear motion. The main kinetic equation in all these approaches is a master equation, or Fokker–Planck equation, for the distribution function of the collective coordinates and the conjugate momenta in the phase space of the collective degrees of freedom. The solution of the Fokker–Planck equation contains information about the mean values and fluctuations of the dynamical variables. At the same time, the mean values satisfy Newton's equation with friction forces.

In single-particle models (Refs. 63, 64, 68, 69, and 72),

the transport coefficients of a Fokker–Planck equation describing transfer of mass, charge, energy, and angular momentum have been obtained. In these models, it is assumed that the reaction partners retain their individuality. The internal system is described as a sum of independent internal subsystems of each of the nuclei. In the model of Refs. 63 and 64, allowance is made for incoherent particle–hole excitations and the exchange of nucleons between nuclei due to nondiagonal matrix elements of the single-particle potential. The model of Refs. 68 and 69 considers only exchange of nucleons and is a microscopic analog of the classical picture of the exchange of particles through a window during the collision of the nuclei ("proximity" model).[49] A statistical hypothesis enters the model together with the assumption of rapid randomization of the motions of the nucleons in each of the nuclei. The simplicity of the model of Refs. 68 and 69 and the success in describing the loss of kinetic energy ("window" formula) and the widths of the mass (charge) distributions of the reaction products are intriguing.

In neither model are the shell effects treated explicitly, and no allowance is made for the details of the single-particle spectra of the reaction partners. In the model of Refs. 63 and 64, the matrix elements for nucleon transfer from nucleus to nucleus are determined by a procedure of averaging over all shell configurations. An influence of the structure of the interacting nuclei is manifested only in a strong dependence of the transport coefficients on the density of the single-particle levels. In the second model the interacting nuclei are treated in the Fermi-gas approximation, and this means that the structure of the nuclei is taken into account only in an averaged manner through the ground-state energy and the parameters of the level density. It should be noted that the transport coefficients obtained in these approaches differ strongly. The approximation of Refs. 63 and 64 is not based on perturbation theory, in contrast to the model of Refs. 68 and 69, in which the coupling between the collective and internal motions is described not in a self-consistent manner but only on the average and in the first order of perturbation theory ("weak-coupling" limit). The transport model of Refs. 68 and 69 includes (classically) dynamical effects, whereas the model of Refs. 63 and 64 does not consider explicitly the relative motion of the nuclei.

In the linear-response theory of Refs. 65 and 66, the main statistical hypothesis is the assumption that at each point of the classical trajectory the internal system is close to thermodynamic equilibrium. It is then possible to calculate the deviation of the density matrix of the internal system from equilibrium by perturbation theory. The linear-response theory is formulated in the quasiadiabatic approximation ("weak-coupling" limit), i.e., the model is valid only for low collective velocities. The excitation of the internal system (incoherent particle–hole excitations in a two-center potential) is generated after each infinitesimally short time interval by a change in the mean field of the dinuclear system. As macroscopic (collective) degrees of freedom, the relative motion of the nuclei, the mass (charge) asymmetry, and the shapes of the nuclei are taken into account in this model. The macroscopic and microscopic degrees of freedom are coupled by a friction tensor. The friction and the diffusion coefficient are connected by Einstein's relation. The dissipation in the framework of linear-response theory is a quantum-mechanical version of the classical single-body friction ("wall" formula).

In all the above-mentioned transport models it is assumed that the dinuclear system is highly excited and that local equilibrium is established during a very short interval of time. This is a good approximation for the final stage of the reaction but is not correct for the description of the initial stage. The calculations of Ref. 6 show that in the initial stage of deep inelastic heavy-ion collisions strong coherent excitations, which decay into complex incoherent states during the time in which local equilibrium is established, are dominant. To take into account these effects, a modified Fokker–Planck equation, in which allowance is made for the nonstatistical initial phase of the collision, was obtained in Ref. 79.

In heavy-ion reactions at an energy a few MeV/nucleon above the Coulomb barrier, the dinuclear system can be characterized in a good approximation as a system consisting of noninteracting particles with a common time-dependent mean field, since the average velocity (Fermi velocity) of the nucleons is much greater than the relative velocity of the ions. For the description of the initial stage of the reaction, the most general microscopic approach is through the solution of the many-particle Schrödinger equation in the time-dependent Hartree–Fock approximation (TDHF).[80–82] The TDHF contains a description of all the degrees of freedom that are considered in the transport models. However, certain problems arise with the separation of these macroscopic observables, owing to the nonlinearity of the dynamical equations. In the framework of the TDHF it is possible to obtain a good description of the fission cross section and deep inelastic collisions, the deflection functions, the dissipation of energy and relative angular momentum, the centroids of the mass (charge) distributions, etc. At the same time, the calculated dispersions of the mass (charge) distributions are several times smaller than the experimental dispersions. The TDHF is also unable to give a good description of the fusion cross section. Another serious shortcoming of the TDHF in the theory of nuclear reactions is its inability to take into account fluctuations of the mean field and, in particular, of its shape. Moreover, the practical realization of the method encounters numerous computational difficulties. There is therefore interest in alternative approaches based on the TDHF such as the adiabatic time-dependent Hartree–Fock approximation (ATDHF) and semimicroscopic hydrodynamic models.[73,82]

The multistage processes of heavy-ion collisions can be described consistently in the framework of the coupled-channel method.[83,84] For simplicity, one usually goes over from the system of equations of this method to a transport equation, and the coupling of the channels is modeled by means of friction forces.[85]

There now exist simple models[86–95] in which one does not take into account all the effects (for example, microscopic self-consistency of the density and nuclear potential) included in the TDHF method. However, by means of them it is possible to make significant progress in understanding the physics of the interaction of nuclei. In the framework of

such an approach, we have attempted to describe in a unified manner heavy-ion collisions in a wide range of energies—from the quasielastic to the deep inelastic regime. Our model (Refs. 52, 76, 77, and 96–108) makes it possible to take into account explicitly the influence of the shell structure of the nuclei on the collision process. Constituent elements of the model are a realistic scheme of single-particle levels, nucleon separation energies, single-particle matrix elements of inelastic transitions of nucleons in the nucleus due to the effect of the field of the incident ion, and the matrix elements of nucleon transfer from nucleus to nucleus. The single-particle approximation is improved by phenomenological allowance for the residual interaction between the nucleons. The model also makes it possible to take into account in a simpler manner the fluctuations associated with the distortion of the mean field in the framework of the random-phase approximation. Knowledge of the evolution of the single-particle degrees of freedom makes it possible to obtain transport coefficients, and this provides a microscopic basis for the phenomenological description of deep inelastic heavy-ion collisions on the basis of a "master" equation or a Fokker–Planck equation.[76,77] On the basis of the explicit evolution operator for the system, we obtained in Refs. 96–101 the probabilities of transitions between macroscopic states of the system differing in the charge (mass) asymmetry. The results of these studies indicate a strong influence of the shell structure on the many-nucleon transfers, i.e., the change in the macroscopic parameters of the dinuclear system is determined by microscopic transitions of nucleons. The reason for the transitions is that after the heavy-ion collision the nucleons are in a certain mean field of the dinuclear system, and their states are no longer eigenstates for the Hamiltonian of the system. Study of the changes of the collective variables of the dinuclear system makes it possible to obtain experimentally observable characteristics of heavy-ion reactions. It is interesting to establish the connection between the macroscopic and microscopic approaches used to describe the evolution of dinuclear systems and, in particular, to develop a method of microscopic calculation of the energy of the dinuclear systems.

1. BASIC PROPOSITIONS OF THE MICROSCOPIC MODEL

The model is based on the assumption that at the considered collision energies the nuclei retain their individual properties. Therefore, for the quantum-mechanical description of the internal degrees of freedom we use a single-particle approximation with realistic schemes of the single-particle levels for each of the nuclei. Qualitatively, the process is represented as follows: Two potential wells (Woods–Saxon potentials) whose centroids move along classical trajectories perturb each other, giving rise to changes in the state of motion of the nucleons and transfers of them from nucleus to nucleus. In this model, this mechanism is the main mechanism of kinetic-energy dissipation and exchange of nucleons. Two-particle collisions of the nucleons are taken into account indirectly through the Fermi (thermal) occupation numbers. Effects associated with the residual interaction like excitation of high- and low-lying collective states of the nuclei and of the dinuclear system are not taken into account explicitly, although the readily excited modes of surface vibrations must contribute to the dissipation. The adiabaticity of the relative motion with respect to these vibrations reduces this effect.

It is convenient to represent the total Hamiltonian $\hat{H}$ of the dinuclear system in the form

$$\hat{H}=\hat{H}_{\rm rel}+\hat{H}_{\rm in}+\hat{V}_{\rm int}. \tag{1}$$

The Hamiltonian

$$\hat{H}_{\rm rel}=\frac{\hat{\mathbf{P}}^2}{2\mu}+U(\hat{\mathbf{R}})$$

of the relative motion is the sum of the kinetic-energy operator and the interaction potential $U(\hat{\mathbf{R}})$ of the nuclei in the ground state. Here, $\hat{\mathbf{R}}$ is the distance between the centers of mass of the fragments, $\hat{\mathbf{P}}$ is the conjugate momentum, and μ is the reduced mass of the system. The last two terms of (1) describe the internal motion of the noninteracting nuclei and the coupling of the relative motion to the internal motion, respectively.

Using Ehrenfest's theorem, it is easy to obtain from (1) the classical limit of the equations of motion for the macroscopic collective variables $\mathbf{R}$ and $\mathbf{P}$:

$$\dot{\mathbf{R}}=\nabla_{\mathbf{P}}(H_{\rm rel}+\langle t|\hat{V}_{\rm int}|t\rangle), \tag{2}$$

$$\dot{\mathbf{P}}=-\nabla_{\mathbf{R}}(H_{\rm rel}+\langle t|\hat{V}_{\rm int}|t\rangle), \tag{3}$$

where the average $\langle t|\ldots|t\rangle$ is over the internal variables at the time t. It can be seen that the classical motion of the nuclei depends additionally on the time-dependent nonconservative coupling potential $\langle t|\hat{V}_{\rm int}|t\rangle$, for the calculation of which it is necessary to consider the equation of motion for the single-particle density matrix.

A single-particle basis is constructed from the asymptotic wave vectors of the single-particle states of the noninteracting nuclei—the incident (projectile) ion "P", $|P\rangle$, and the target nucleus "T", $|T\rangle$, in the form

$$|\tilde{P}\rangle=|P\rangle-\tfrac{1}{2}\sum_{T}|T\rangle\langle T|P\rangle,$$

$$|\tilde{T}\rangle=|T\rangle-\tfrac{1}{2}\sum_{P}|P\rangle\langle P|T\rangle.$$

For this basis set, the orthogonality condition is satisfied up to terms of second order in the overlap integral $\langle P|T\rangle$.[52]

It is convenient to take the single-particle Hamiltonian $\hat{\mathscr{H}}$ of the dinuclear system in the form

$$\hat{\mathscr{H}}(\mathbf{R}(t))=\sum_{i=1}^{A}\left(\frac{-\hbar^2}{2m}\Delta_i+U_P(\mathbf{r}_i-\mathbf{R}(t))+U_T(\mathbf{r}_i)\right), \tag{4}$$

where m is the nucleon mass, and $A=A_P+A_T$ is the total atomic mass of the system. The mean single-particle potentials of the projectile, U_P, and of the target nucleus, U_T, include both nuclear and Coulomb fields. In the second-quantization representation, the Hamiltonian (4) can be written in the form

$$\hat{\mathscr{H}}(\mathbf{R}(t))=\hat{\tilde{H}}_{\text{in}}(\mathbf{R}(t))+\hat{V}_{\text{int}}(\mathbf{R}(t)),$$

$$\hat{\mathscr{H}}(\mathbf{R}(t))=\sum_i \hat{\varepsilon}_i(\mathbf{R}(t))a_i^+a_i=\sum_P \tilde{\varepsilon}_P(\mathbf{R}(t))a_P^+a_P$$

$$+\sum_T \tilde{\varepsilon}_T(\mathbf{R}(t))a_T^+a_T,$$

$$\hat{V}_{\text{int}}(\mathbf{R}(t))=\sum_{i\neq i'} V_{ii'}(\mathbf{R}(t))a_i^+a_{i'}=\sum_{P\neq P'} \chi_{PP'}^{(T)}$$

$$\times(\mathbf{R}(t))a_P^+a_{P'}+\sum_{T\neq T'} \chi_{TT'}^{(P)}(\mathbf{R}(t))a_T^+a_{T'}$$

$$+\sum_{T,P} g_{PT}(\mathbf{R}(t))(a_P^+a_T+\text{h.c.}). \tag{5}$$

where, up to quantities of second order in the overlap integral $\langle P|T\rangle$,

$$\tilde{\varepsilon}_P(\mathbf{R}(t))=\varepsilon_P+\langle P|U_T(\mathbf{r})|P\rangle,$$

$$\tilde{\varepsilon}_T(\mathbf{R}(t))=\varepsilon_T+\langle T|U_P(\mathbf{r}-\mathbf{R}(t))|T\rangle,$$

$$\chi_{PP'}^{(T)}(\mathbf{R}(t))=\langle P|U_T(\mathbf{R})|P'\rangle,$$

$$\chi_{TT'}^{(P)}(\mathbf{R}(t))=\langle T|U_P(\mathbf{r}-\mathbf{R}(t))|T'\rangle,$$

$$g_{PT}(\mathbf{R}(t))=\tfrac{1}{2}\langle P|U_P(\mathbf{r}-\mathbf{R}(t))+U_T(\mathbf{r})|T\rangle. \tag{6}$$

In the expression (6), $\varepsilon_{P(T)}$ are the energies of the unperturbed single-particle states, which are characterized by the set of quantum numbers $P\equiv(n_P,j_P,l_P,m_P)$ $[T\equiv(n_T,j_T,l_T,m_T)]$. The diagonal matrix elements $\langle P|U_T|P\rangle$ and $\langle T|U_P|T\rangle$ characterize the shifts of the energies of the single-particle levels due to the interaction of the nuclei. The nondiagonal matrix elements $\chi_{PP'}^{(T)}$ and $\chi_{TT'}^{(P)}$ correspond to particle–hole transitions between levels in one of the nuclei under the influence of the mean field of the partner nucleus. In their turn, the g_{PT} determine transitions of the nucleons from nucleus to nucleus because of the action of the mean field of the dinuclear system. The contributions to the matrix elements from noninertial effects are not taken into account, since they are small.[91] Information about the evolution of the system can be obtained by solving the equation of motion for the single-particle density matrix. If one is only interested in the charge (mass) distribution of the products of the deep inelastic heavy-ion collisions, it is possible to use directly the kinetic equation for the probability of finding the system in a definite state.

2. DISTRIBUTION OF EXCITATION ENERGY BETWEEN THE REACTION PRODUCTS

Dissipation of the kinetic energy

The large loss of kinetic energy in deep inelastic heavy-ion collisions is one of the characteristic features of this type of nuclear reaction.[1,6] It was originally assumed that the kinetic energy of the relative motion, which is transformed into energy of internal excitation, is distributed between the fragments in proportion to their masses (thermodynamic equilibrium). However, it was shown later in a number of experiments that this assumption is not correct. In some reactions, the excitation energy is distributed approximately equally between the products of binary reactions.[25,26,109] In other reactions,[27–33] the distribution of the excitation energy is intermediate between an equal distribution and one proportional to the masses of the nuclei. In the reactions with ^{52}Cr+^{208}Pb (Ref. 34), ^{238}U+^{124}Sn, ^{110}Pd (Ref. 35) most of the excitation energy is concentrated in the light product at relatively large losses of the kinetic energy. These new experimental data stimulated a growth of interest in the problem of kinetic-energy dissipation, since knowledge of the distribution of the excitation energy between the fragments is needed to recover the initial yield of the reaction products from the measured yields of evaporated remnants.

Calculation of the friction forces requires the formulation of a microscopic model that treats explicitly the coupling of the relative motion to the internal motion (Refs. 86–95 and 110–112). The models differ in the internal excitations that are considered. They may be collective surface vibrations, giant resonances, incoherent particle–hole excitations corresponding to inelastic excitations of the interacting nuclei, or transitions of nucleons from nucleus to nucleus. It is clear that the structure of the excited states of the nuclei and the strength of the coupling of the various excitation modes to the relative motion will influence the energy distribution between the fragments.

The equation of motion for the single-particle density matrix $\hat{n}(t)$,

$$i\hbar\frac{\partial\hat{n}(t)}{\partial t}=[\hat{\mathscr{H}}(\mathbf{R}(t)),\hat{n}(t)], \tag{7}$$

has, in the matrix representation, the form

$$i\hbar\frac{dn_i(t)}{dt}=\sum_k [V_{ik}(\mathbf{R}(t))n_{ki}(t)-n_{ik}(t)V_{ki}(\mathbf{R}(t))], \tag{8}$$

$$i\hbar\frac{dn_{ik}(t)}{dt}=\hbar\tilde{\omega}_{ik}(\mathbf{R}(t))n_{ik}(t)+V_{ki}(\mathbf{R}(t))$$

$$\times[n_k(t)-n_i(t)], \tag{9}$$

where we have used the notation $\tilde{\omega}_{ik}=[\tilde{\varepsilon}_i-\tilde{\varepsilon}_k]/\hbar$, $n_{ik}(t)=\langle t|a_i^+a_k|t\rangle$, $n_i(t)=n_{ii}(t)=\langle t|a_i^+a_i|t\rangle$. In the expression (9) we can make the simplification (random-phase approximation)

$$\sum_k V_{k'i}(\mathbf{R}(t))n_{k'k}(t)-\sum_{i'} V_{ki'}(\mathbf{R}(t))n_{ii'}(t)$$

$$\approx V_{ki}(\mathbf{R}(t))[n_k(t)-n_i(t)]. \tag{10}$$

Then, substituting the solution

$$n_{ik}(t)=\frac{1}{i\hbar}\int_{t_0}^{t}dt'V_{ik}(\mathbf{R}(t'))\exp\left\{i\int_{t'}^{t}dt''\tilde{\omega}_{ki}(\mathbf{R}(t''))\right\}$$

$$\times[n_k(t')-n_i(t')] \tag{11}$$

of (9) in the expression (8), we obtain for the dynamical occupation numbers $n_i(t)$ the equation

$$\frac{dn_i(t)}{dt}=\sum_k \int_{t_0}^{t} dt' \Omega_{ik}(t,t')[n_k(t')-n_i(t')] \tag{12}$$

where

$$\Omega_{ik}(t,t')=\frac{2}{\hbar^2}\,\mathrm{Re}\left\{ V_{ik}(\mathbf{R}(t))V_{ki}(\mathbf{R}(t')) \times\exp\left[i\int_{t'}^{t} dt''\tilde{\omega}_{ki}(\mathbf{R}(t''))\right]\right\}.$$

Equation (12) resembles in its structure a master equation, but, in contrast to such an equation, it takes into account "memory" effects by virtue of its integral nature. The process of intense excitation of the nuclei affects a large number of single-particle states, and the occupation numbers $n_i(t)$ corresponding to them change very slowly with the time. In addition, the kernel of the integro-differential equation (12) has a sharp maximum at $t'=t$. Therefore, Eq. (12) can be written in the form

$$\frac{dn_i(t)}{dt}=\sum_k w_{ik}(t,t_0)(n_k(t)-n_i(t)), \tag{13}$$

where

$$w_{ik}(t,t_0)=\int_{t_0}^{t} dt' \Omega_{ik}(t,t').$$

The "master" equation (13) can be solved by successive iteration:

$$n_i(t+\Delta t)=n_i(t)+\sum_k \bar{W}_{ik}(\mathbf{R}(t),\Delta t)[n_k(t)-n_i(t)],$$

$$\bar{W}_{ik}(\mathbf{R}(t),\Delta t)=|V_{ik}(\mathbf{R}(t))|^2\frac{\sin^2\left(\frac{\Delta t}{2}\tilde{\omega}_{ki}(\mathbf{R}(t))\right)}{\left[\frac{\hbar}{2}\tilde{\omega}_{ki}(\mathbf{R}(t))\right]^2}. \tag{14}$$

The occupation numbers at the initial time are taken to be equal to unity for occupied states and zero for free states.

Equation (13) describes an irreversible evolution of the system. Indeed, with allowance for Eq. (13) and the definition of the entropy $S(t)$ of the nonequilibrium system in terms of the occupation numbers,

$$S(t)=-k\sum_i [n_i(t)\ln n_i(t)+\bar{n}_i(t)\ln \bar{n}_i(t)],$$

$$\bar{n}_i(t)=1-n_i(t), \tag{15}$$

(k is Boltzmann's constant), we find that the time derivative

$$\frac{dS(t)}{dt}=\frac{k}{2}\sum_{i,k} w_{ik}(t,t_0)(n_i(t)\bar{n}_k(t) -n_k(t)\bar{n}_i(t))\ln\left[\frac{n_i(t)\bar{n}_k(t)}{\bar{n}_i(t)n_k(t)}\right] \tag{16}$$

of the entropy is non-negative, i.e., the entropy increases with the time, or is equal to zero in the equilibrium state. This proves the irreversibility of Eqs. (12) and (13), which arises because of the loss of information about the process resulting from the assumptions that it is a Markov process and that $\hat{V}$ and $\hat{n}$ are random [see (10)].

In the process of the reaction, there is, simultaneously with the general heating of the nucleus, relaxation of the system to a statistically equilibrium state. However, the steady solution of Eqs. (12) and (13) does not give in the asymptotic limit ($t\to\infty$) for fixed R the Fermi thermal occupation numbers, since we have not taken into account from the beginning the residual interaction between the nucleons. Allowance for them in the Hamiltonian (1) leads to the appearance, on the right-hand side of Eqs. (12) and (13), of the well-known two-particle collision term,[113,114] in addition to the single-particle term:

$$\sum_{jkl}\int_{t_0}^{t} dt' \Omega^{\mathrm{res}}_{ijkl}(t,t')[\bar{n}_i(t')\bar{n}_j(t')n_k(t')n_l(t') -n_i(t')n_j(t')\bar{n}_i(t')\bar{n}_j(t')],$$

$$\Omega^{\mathrm{res}}_{ijkl}(t,t')=\frac{1}{h^2}\,\mathrm{Re}\left\{ V^{\mathrm{res}}_{ijkl}(\mathbf{R}(t))V^{\mathrm{res}}_{lkji}(\mathbf{R}(t')) \times\exp\left[i\int_{t'}^{t} dt''\tilde{\omega}_{lkji}(\mathbf{R}(t''))\right]\right\},$$

where $\tilde{\omega}_{lkji}=[\tilde{\varepsilon}_l+\tilde{\varepsilon}_k-\tilde{\varepsilon}_j-\tilde{\varepsilon}_i]/h$, and V^{res}_{ijkl} is the matrix element of the residual interaction. The indices range over all the single-particle states of the projectile P and the target nucleus T.

It is then possible to calculate the time derivative of the entropy with allowance for the two-particle collision term:

$$\frac{dS(t)}{dt}=\frac{k}{2}\left\{\sum_{i,k} w_{ik}(t,t_0)(n_i\bar{n}_k-n_k\bar{n}_i)\ln\left[\frac{n_i\bar{n}_k}{n_k\bar{n}_i}\right] +\tfrac{1}{2}\sum_{ijkl} w^{\mathrm{res}}_{ijkl}(t,t_0)[n_in_j\bar{n}_k\bar{n}_l -\bar{n}_i\bar{n}_jn_kn_l]\ln\left[\frac{n_in_j\bar{n}_k\bar{n}_l}{\bar{n}_i\bar{n}_jn_kn_l}\right]\right\}, \tag{17}$$

where we have used the notation $n_i=n_i(t)$, $\bar{n}_i-n_i(t)$, and

$$w^{\mathrm{res}}_{ijkl}(t,t_0)=\int_{t_0}^{t} dt' \Omega^{\mathrm{res}}_{ijkl}(t,t').$$

It is known that the steady solution of Eq. (17) corresponds to an equilibrium distribution with temperature-dependent occupation numbers of Fermi type and that the Fermi energies and the temperatures of the nuclei are equal to each other: $\varepsilon_{F_P}=\varepsilon_{F_T}, T_P=T_T$.

Explicit allowance for the residual interaction requires extensive calculations. It is therefore customary to take into account the two-particle collision integral in linearized form (τ approximation).[115,116] Then the equation for the single-particle density matrix $\hat{\bar{n}}$ takes the form

$$ih\frac{\partial\hat{\bar{n}}(t)}{\partial t}=[\hat{\mathscr{H}},\hat{\bar{n}}(t)]-\frac{i\hbar}{\tau}\{\hat{\bar{n}}(t)-\hat{\bar{n}}^{\mathrm{eq}}(\mathbf{R}(t))\}, \tag{7'}$$

where τ is the time parameter of the relaxation, and $\tilde{n}^{eq}(\mathbf{R}(t))$ is the local quasiequilibrium distribution, i.e., the equilibrium distribution for a fixed value of the collective coordinate $\mathbf{R}$.

As for the expressions (8), (9), (11), and (12), we obtain the equations

$$i\hbar \frac{d\tilde{n}_i(t)}{dt} = \sum_k [V_{ik}(\mathbf{R}(t))\tilde{n}_{ki}(t) - V_{ki}(\mathbf{R}(t))\tilde{n}_{ik}(t)] - \frac{i\hbar}{\tau}[\tilde{n}_i(t) - \tilde{n}_i^{eq}(\mathbf{R}(t))], \quad (8')$$

$$i\hbar \frac{d\tilde{n}_{ik}(t)}{dt} = \hbar\left[\tilde{\omega}_{ik}(\mathbf{R}(t)) - \frac{2i}{\tau}\right]\tilde{n}_{ik}(t) + V_{ki}(\mathbf{R}(t)) \times [\tilde{n}_k(t) - \tilde{n}_i(t)], \quad (9')$$

$$\tilde{n}_{ik}(t) = \frac{1}{i\hbar}\int_{t_0}^{t} dt' V_{ik}(\mathbf{R}(t'))\exp\left\{i\int_{t'}^{t} dt''\left[\tilde{\omega}_{ki}(\mathbf{R}(t'')) + \frac{2i}{\tau}\right]\right\}[\tilde{n}_k(t') - \tilde{n}_i(t')], \quad (11')$$

$$\frac{d\tilde{n}_i(t)}{dt} = \sum_k \int_{t_0}^{t} dt' \Omega_{ik}(t,t')\exp\left(\frac{t'-t}{\tau/2}\right) \times [\tilde{n}_k(t') - \tilde{n}_i(t')] - \frac{1}{\tau}[\tilde{n}_i(t) - \tilde{n}_i^{eq}(\mathbf{R}(t))]. \quad (12')$$

The formal solution of Eq. (12′) has the form

$$\tilde{n}_i(t) = \exp\left(\frac{t_0 - t}{\tau}\right)\left\{\tilde{n}_i(t_0) + \sum_k \int_{t_0}^{t} dt' \int_{t_0}^{t'} dt'' \Omega_{ik}(t',t'')\exp\left(\frac{t''-t}{\tau/2}\right) \times [\tilde{n}_k(t'') - \tilde{n}_i(t'')] + \frac{1}{\tau} + \int_{t_0}^{t} dt' \tilde{n}_i^{eq}(\mathbf{R}(t'))\exp\left(\frac{t'-t_0}{\tau}\right)\right\}. \quad (18)$$

It is convenient to solve Eq. (18) iteratively, dividing the time interval $(t - t_0)$ into subintervals: t_0, $t_0 + \Delta t$, $t_0 + 2\Delta t$, etc. Then for times $\Delta t < \tau$, Eq. (18) can be written approximately as

$$\tilde{n}_i(t) = \tilde{n}_i^{eq}(\mathbf{R}(t))\left[1 - \exp\left(\frac{-\Delta t}{\tau}\right)\right] + n_i(t)\exp\left(\frac{-\Delta t}{\tau}\right),$$

$$n_i(t) = \tilde{n}_i(t - \Delta t) + \sum_k \tilde{W}_{ik}(\mathbf{R}(t), \Delta t)[\tilde{n}_k(t - \Delta t) - \tilde{n}_i(t - \Delta t)], \quad (19)$$

where $\tilde{W}_{ik}$ is defined in (14). The dynamical, $n_i(t)$, and quasiequilibrium (thermal), $\tilde{n}_i^{(eq)}(\mathbf{R}(t))$, occupation numbers are calculated in each iterative step Δt. The parameters of the Fermi distribution for the proton and neutron subsystems of each of the nuclei are determined by the conservation laws for the energy and nucleon numbers of each type.

The relative contributions of the single- and two-particle components are determined by the value of the relaxation time τ, which is the only parameter of our model.

Knowing the values of the occupation numbers $\tilde{n}_i(t)$, we can readily determine at any time t the mean numbers of protons, $Z_{P(T)}$, and of neutrons, $N_{P(T)}$, and their variances σ_Z^2 or σ_N^2 for each of the nuclei, and we can also find the fragment excitation energies $E^*_{P,T}(t)$:

$$Z_{P(T)}(t) = \sum_{P(T)}^{Z} \tilde{n}_{P(T)}(t), \quad (20)$$

$$N_{P(T)}(t) = \sum_{P(T)}^{N} \tilde{n}_{P(T)}(t), \quad (21)$$

$$\sigma^2_{Z(N)}(t) = \sum_{P}^{Z(N)} \tilde{n}_P(t)[1 - \tilde{n}_P(t)], \quad (22)$$

$$E^*_{P(T)}(t) = \sum_{P(T)} [\tilde{\varepsilon}_{P(T)}(\mathbf{R}(t)) - \varepsilon_{F_{P(F_T)}}(\mathbf{R}(t))][\tilde{n}_{P(T)}(t) - \tilde{n}_{P(T)}(t_0)], \quad (23)$$

where $\varepsilon_{F_{P(F_T)}}(\mathbf{R}(t))$ is the Fermi energy of the light, P, and heavy, T, fragment. The upper indices Z and N of the sum indicate summation over the proton and neutron single-particle levels, respectively. In each iterative step, we must separate the contribution to the fragment excitation energy from the particle–hole excitations and from the exchange of nucleons.

Transport coefficients

Substituting (11′) in (3), we obtain the integro-differential equation

$$\frac{d}{dt}[\mu(\mathbf{R}(t))\dot{\mathbf{R}}(t)] = -\nabla_{\mathbf{R}} U(\mathbf{R}(t)) - 2\,\mathrm{Re}\sum_{i \neq k} \nabla_{\mathbf{R}} V_{ki}(\mathbf{R}(t))\tilde{n}_{ik}(t). \quad (24)$$

The second term on the right-hand side of (24) contains effective forces, of both conservative and dissipative nature, due to the coupling of the relative motion with the internal motion. This term depends explicitly not only on the relative separation $R(t)$ but also on the current time t, in contrast to linear-response theory, in which the asymptotic values are taken.[65]

In the adiabatic limit, when the characteristic time of the collective motion is much greater than the relaxation time, we can expand the function $V_{ki}(\mathbf{R}(t'))$ in Eq. (24) near the point $t' = t$:

$$V_{ik}(\mathbf{R}(t')) = V_{ik}(\mathbf{R}(t)) + (t' - t)\dot{\mathbf{R}}(t)\nabla_{\mathbf{R}} V_{ik}(\mathbf{R}(t))$$

$$+\frac{(t'-t)^2}{2}\ddot{\mathbf{R}}(t)\nabla_{\mathbf{R}}V_{ik}(\mathbf{R}(t))$$

$$+\frac{(t'-t)^2}{2}(\dot{\mathbf{R}}(t)\nabla_{\mathbf{R}})^2V_{ik}(\mathbf{R}(t))+\dots\ .$$

The first term of the expansion gives the dynamical correction $\nabla_{\mathbf{R}}\delta U(\mathbf{R}(t))$ to the conservative force $\nabla_{\mathbf{R}}U(\mathbf{R}(t))$:

$$-\nabla_{\mathbf{R}}\delta U(\mathbf{R}(t))=\sum_{ik}V_{ik}(\mathbf{R}(t))\nabla_{\mathbf{R}}V_{ki}(\mathbf{R}(t))B_{ik}^{(0)}(t,t_0)$$

$$\times[\tilde{n}_i(t)-\tilde{n}_k(t)],$$

where

$$B_{ik}^{(n)}(t,t_0)=\frac{2}{\hbar}\int_{t_0}^{t}dt'\,\frac{(t'-t)^n}{n!}\exp\left(\frac{t'-t}{\tau/2}\right)$$

$$\times\sin\{\tilde{\omega}_{ki}(\mathbf{R}(t))[t-t']\}.$$

One can similarly write down the correction $\delta U(\mathbf{R}(t))$ to the conservative potential $U(\mathbf{R}(t))$ due to the particle–hole excitations and the exchange of nucleons:

$$\delta U(\mathbf{R}(t))=\tfrac{1}{2}\sum_{ik}|V_{ik}(\mathbf{R}(t))|^2B_{ik}^{(0)}(t,t_0)[\tilde{n}_k(t)-\tilde{n}_i(t)].$$

Allowance for the second term leads to an irreversible loss of kinetic energy of the relative motion, which is expended on internal excitation of the nuclei. The coefficients of radial and tangential friction, respectively, can be written in the form

$$k_R(R(t))=\sum_{ik}\left|\frac{\partial V_{ik}(\mathbf{R}(t))}{\partial R}\right|^2B_{ik}^{(1)}(t,t_0)[\tilde{n}_k(t)-\tilde{n}_i(t)],$$

$$k_T(R(t))=\frac{1}{2(R(t))^2}\sum_{ik,L}L(L+1)|V_{ik}^L(\mathbf{R}(t))|^2B_{ik}^{(1)}$$

$$\times(t,t_0)(\tilde{n}_k(t)-\tilde{n}_i(t)),$$

where

$$V_{ik}(\mathbf{R}(t))=\sum_{L=|l_k-l_i|}^{l_k+l_i}V_{ik}^L(\mathbf{R}(t))$$

and $V_{ik}^L(\mathbf{R}(t))$ is the partial form factor for the given angular-momentum transfer L.[102]

The third term gives the correction

$$\Delta\mu(\mathbf{R}(t))=2\sum_{ik}|\nabla_{\mathbf{R}}V_{ik}(\mathbf{R}(t))|^2B_{ki}^{(2)}(t,t_0)$$

$$\times[\tilde{n}_k(t)-\tilde{n}_i(t)]$$

to the reduced mass $\mu(\mathbf{R}(t))$.

One can calculate similarly the transport coefficients for the other microscopic collective variables such as the mass (charge) asymmetry and the deformation of the nuclei of the dinuclear system.

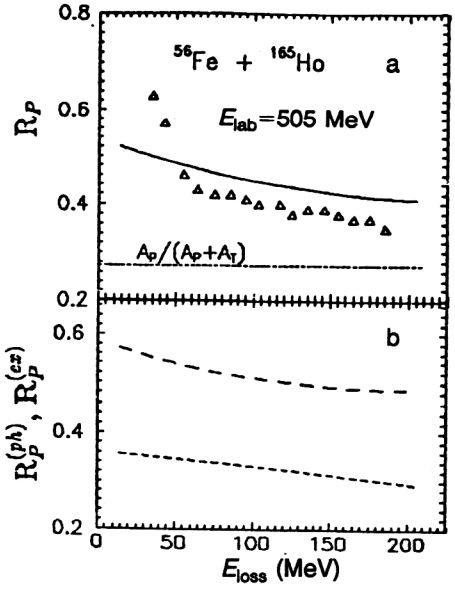

FIG. 1. a) Ratio R_P of the excitation energy (E_P^*) of the fragment corresponding to the projectile nucleus to the total excitation energy E_{loss} = E_P^* + E_T^* of the system as a function of the total energy E_{loss} for the ^{56}Fe(505 MeV)+^{165}Ho reaction. The triangles represent experimental results. The solid continuous curve is calculated in accordance with our model, and the dotted curve is the limit of thermal equilibrium [E_P^*/E_{loss} = $A_P/(A_P + A_T)$]. b) Dependences of the calculated ratios $R_P^{(ex)}$ = $E_P^{*(ex)}/(E_P^{*(ex)} + E_T^{*(ex)})$ (curve with long dashes) and $R_P^{(ph)}$ = $E_P^{*(ph)}/(E_P^{*(ph)} + E_T^{*(ph)})$ (short dashes) for the same reaction.

Results of calculations

To demonstrate the possibilities of the model, we calculated the distribution of the excitation energy between the products of deep inelastic heavy-ion collisions in the reactions ^{238}U(1468 MeV)+^{124}Sn, ^{238}U(1398 MeV)+^{110}Pd (Ref. 35), ^{56}Fe(505 MeV)+^{165}Ho (Refs. 27–29), ^{74}Ge(629 MeV)+^{165}Ho (Refs. 30–33), and ^{58}Ni(880 MeV)+^{197}Au

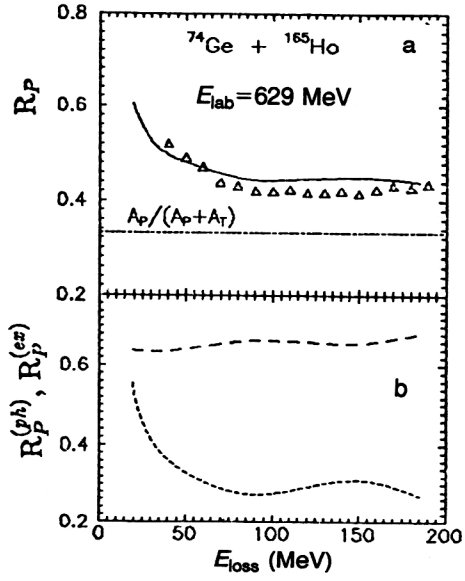

FIG. 2. The same as in Fig. 1 but for the ^{74}Ge(629 MeV)+^{165}Ho reaction.

TABLE I. Calculated ratio of the excitation energy $E_{\text{loss}}^{\text{ph}} = E_P^{*(\text{ph})} + E_T^{*(\text{ph})}$ associated with particle–hole excitations to the energy $E_{\text{loss}}^{\text{ex}} = E_P^{*(\text{ex})} + E_T^{*(\text{ex})}$ due to nucleon exchange for various values of the angular momentum J.

Reaction	E_{lab} (MeV)	J	$E_{\text{loss}}^{(\text{ph})}/E_{\text{loss}}^{(\text{ex})}$
^{238}U+^{110}Pd	1398	57	0.70
^{238}U+^{124}Sn	1468	50	0.67
^{238}U+^{124}Sn	1468	100	0.60
^{58}Ni+^{197}Au	880	240	0.18
^{74}Ge+^{165}Ho	629	169	0.30
^{56}Fe+^{165}Ho	505	175	0.31

(Ref. 26). We investigated the relative importance of nucleon exchange and particle–hole excitations in the process of dissipation of the kinetic energy of the relative motion. The theoretical and experimental results for the ratio of the excitation energy of the projectile nucleus to the total excitation energy of the dinuclear system, $R_P = E_P^*/(E_P^* + E_T^*)$, are shown in Figs. 1a and 2a. For the ^{238}U+^{124}Sn, ^{110}Pd and ^{58}Ni+^{197}Au reactions the mean experimental values of the considered ratios are approximately 0.4 and 0.5, respectively. The results of the calculations, which agree qualitatively with the experimental data, show that the kinetic energy is distributed approximately equally between the fragments, and not in proportion to their masses. The relative importances of nucleon exchange, $R_P^{\text{ex}} = E_P^{*(\text{ex})}/(E_P^{*(\text{ex})} + E_T^{*(\text{ex})})$, and particle–hole excitations, $R_P^{\text{ph}} = E_P^{*(\text{ph})}/(E_P^{*(\text{ph})} + E_T^{*(\text{ph})})$, in the distribution of the excitation energy in the system are characterized by the results given in Figs. 1b, 2b, 3b, 4b, and 5b. Here, $E_{P(T)}^{*(\text{ex})}$ and $E_{P(T)}^{*(\text{ph})}$ are the contributions to $E_{P(T)}^*$ from nucleon exchange and from particle–hole excitations, respectively.

The theoretical results for the ratio of the excitation energy $E_{\text{loss}}^{\text{ph}} = E_P^{*(\text{ph})} + E_T^{*(\text{ph})}$ associated with the particle–hole excitations to the energy $E_{\text{loss}}^{\text{ex}} = E_P^{*(\text{ex})} + E_T^{*(\text{ex})}$ due to nucleon exchange are given in Table I. It can be seen that in the reactions with ^{58}Ni, ^{74}Ge, and ^{56}Fe nucleon exchange plays the main role in the dissipation of the kinetic energy. In reactions with heavier nuclei, the importance of the particle–hole mechanism increases. The mean values of the charge (mass) distributions of the reaction products and their variances are shown in Figs. 6–12. The theoretical dependences agree with the experimental data.

The trajectories of the relative motion of the colliding nuclei were calculated as in Refs. 43 and 117. The single-particle matrix elements $\chi_{TT'}^{(P)}$, $\chi_{PP'}^{(T)}$, and g_{PT} were determined analytically in the approximation proposed in Refs. 77 and 102 (see the Appendix). The calculations showed that variation of the single free parameter τ from $5\cdot10^{-23}$ s to $25\cdot10^{-22}$ s does not have a significant influence on the distribution of the excitation energy between the fragments. All the calculations were made for $\tau = 15\cdot10^{-22}$ s.

The presented results show that the redistribution of the excitation energy between the fragments takes place throughout the interaction of the nuclei, and not only in the initial stage of the reaction. Nucleon exchange, in particular neutron exchange, is the main mechanism of dissipation of the kinetic energy of the relative motion. For heavy systems, the contribution to the excitation energy of the particle–hole excitations becomes comparable to that of the exchange mechanism. The influence of the shell structure of the two interacting nuclei on the exchange of nucleons and on the distribution of the excitation energy between the reaction products is important.

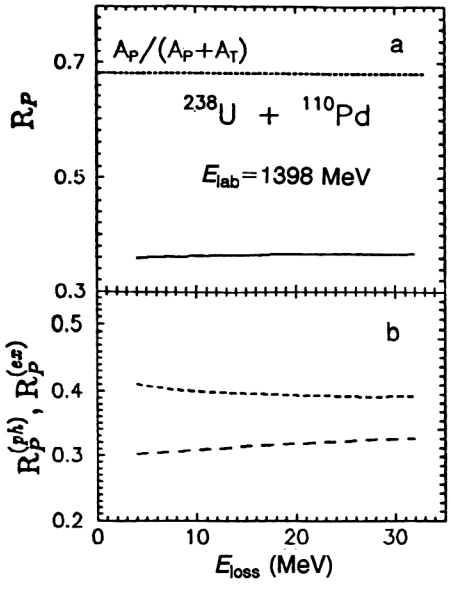

FIG. 3. The same as in Fig. 1 but for the ^{238}U(1398 MeV)+^{110}Pd reaction.

3. INFLUENCE OF SHELL EFFECTS ON NUCLEON TRANSFER IN DEEP INELASTIC HEAVY-ION COLLISIONS

Kinetic approach to the description of deep inelastic heavy-ion collisions

Many of the experimental results listed in the Introduction have not yet been explained in the framework of the

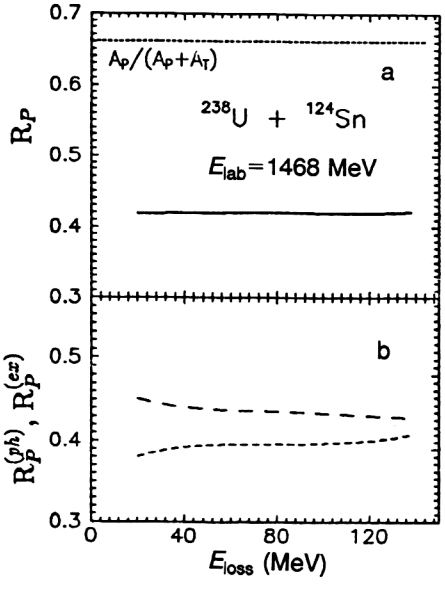

FIG. 4. The same as in Fig. 1 but for the ^{238}U(1468 MeV)+^{124}Sn reaction.

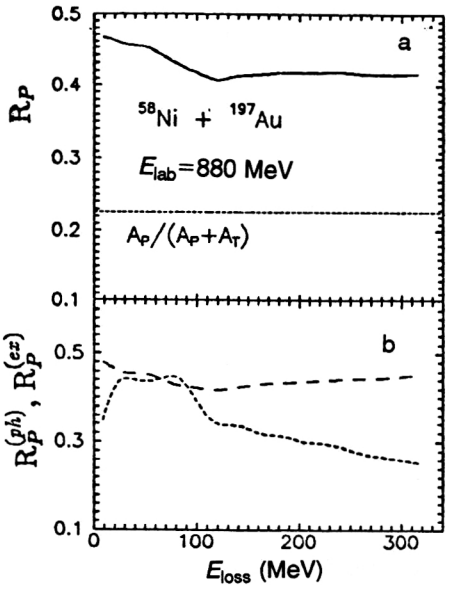

FIG. 5. The same as in Fig. 1 but for the ^{58}Ni(880 MeV)+^{197}Au reaction.

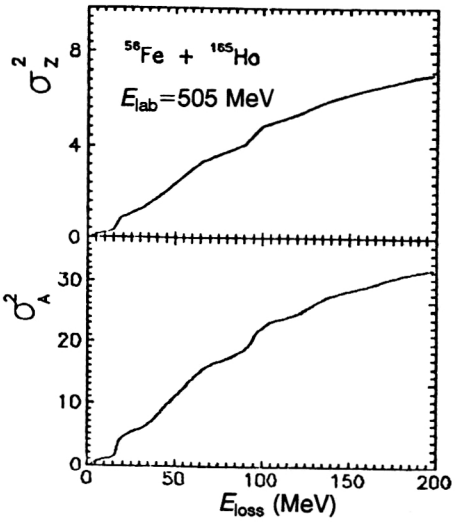

FIG. 7. Variances of the Z_P and A_P distributions as functions of E_{loss} for the ^{56}Fe(505 MeV)+^{165}Ho reaction. The meaning of the symbols in the same as in Fig. 6.

existing models proposed for the description of the charge and mass distributions of the products of deep inelastic heavy-ion collisions. In our view, their interpretation requires allowance for shell effects.

Shell effects are either completely absent in the existing models of heavy-ion reactions or enter them only through the nuclear binding energies. For example, in Nörenberg's model,[63,64] the matrix element of nucleon transition from nucleus to nucleus is determined by means of a procedure of averaging over all shell configurations and therefore does not contain shell effects. It is only in the potential energy of the dinuclear system that one can include the experimental binding energies of the nuclei, which, of course, include shell effects. The shell effects occur explicitly in the calculations of the transition matrix elements in the approach developed in Refs. 96–102.

We investigate the reaction mechanism of many-nucleon transfers, considering the dinuclear system after a large fraction of the kinetic energy has been dissipated and assuming that thermal equilibrium has been established. We shall de-

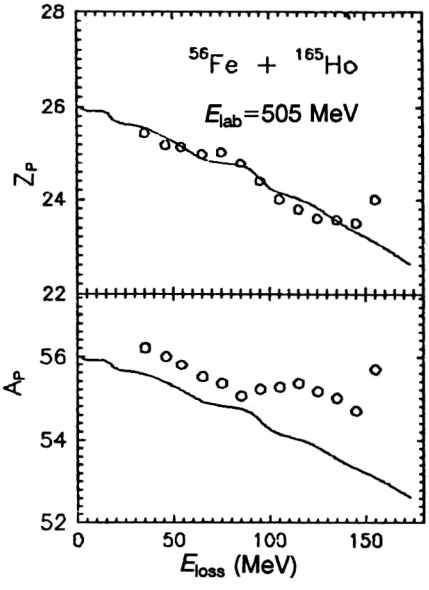

FIG. 6. Centroids of the Z_P and A_P distributions as functions of E_{loss} for the ^{56}Fe(505 MeV)+^{165}Ho reaction. The open circles show the pre-evaporation experimental values. The results of calculations in accordance with the models of Refs. 68 and 69 and our model are shown by the dashed and solid continuous curves, respectively.

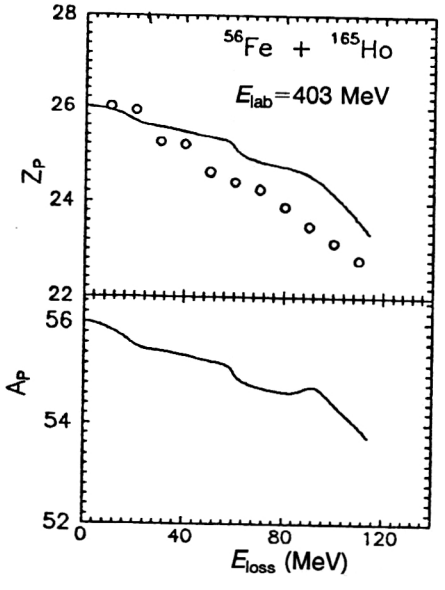

FIG. 8. The same as in Fig. 6 but for the ^{56}Fe(403 MeV)+^{165}Ho reaction.

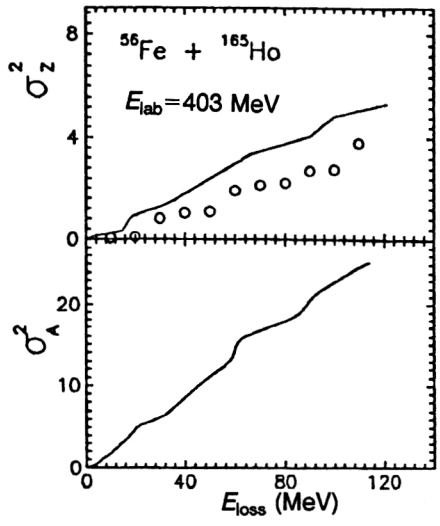

FIG. 9. The same as in Fig. 7 but for the ^{56}Fe(403 MeV)+^{165}Ho reaction.

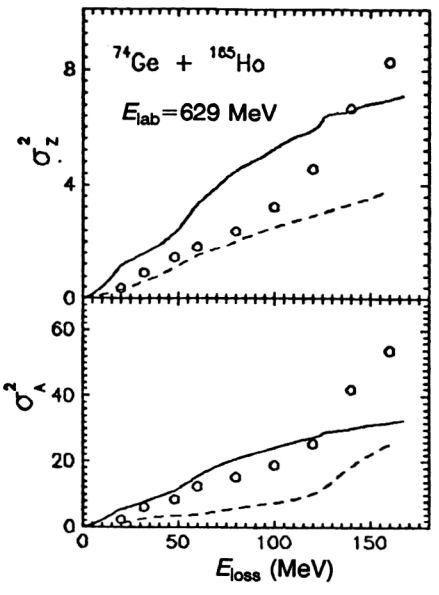

FIG. 11. The same as in Fig. 7 but for the ^{74}Ge(629 MeV)+^{165}Ho reaction.

scribe the subsequent evolution of the system by means of the Hamiltonian (5), ignoring the terms due to particle–hole transitions in the nuclei. Then for the operator $\hat{V}_{\text{int}}$ we have

$$\hat{V}_{\text{int}}=\sum_{P,T}\left(g_{PT}a_T^+a_P+\text{h.c.}\right),$$

which can be rewritten in the form

$$\hat{V}_{\text{int}}=\sum_{k\neq k'=1,2}V_{kk'},\quad V_{12}=\sum_{P,T}g_{PT}a_T^+a_P.$$

The omitted nondiagonal matrix elements in (5) give rise to transitions of nucleons between single-particle levels in one nucleus. This leads to a certain smearing of the Fermi surface. It is assumed that this effect can be taken into account by introducing temperature-dependent occupation numbers $n_P(T)$ and $n_T(T)$. The temperature T is determined by the excitation energy of the system.

At the considered collision energies, the use of the single-particle approximation to describe the reactions is fully justified. This approach presupposes that in the stage of evolution of the system the nuclei retain their individuality, since their overlap is relatively small.[5,6]

The dinuclear system is characterized by its total energy E and charge asymmetry Z. We also consider additional quantum numbers n, which distinguish the states of the dinuclear system for fixed values of E and Z. We denote by $P_Z(n,t)$ the probability of finding the system at the time t in the state with Z and n. The energy E of the system is given.

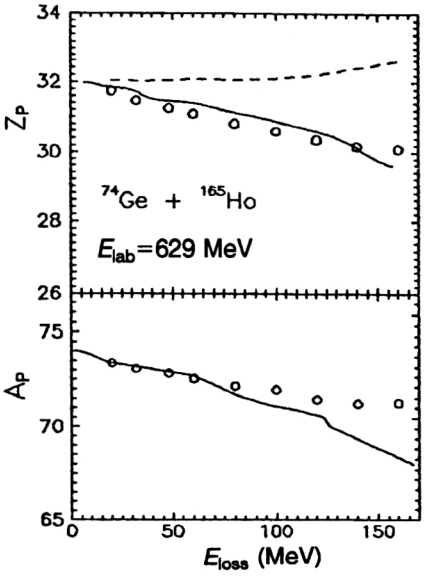

FIG. 10. The same as in Fig. 6 but for the ^{74}Ge(629 MeV)+^{165}Ho reaction.

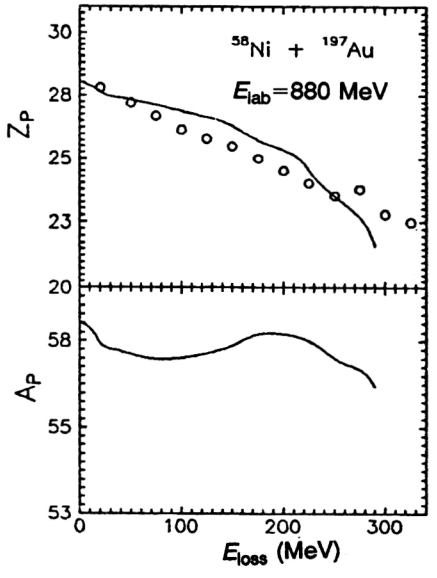

FIG. 12. The same as in Fig. 6 but for the ^{58}Ni(880 MeV)+^{197}Au reaction.

We shall assume that the kinetic approach is valid for the description of many-nucleon transfer reactions[61,71,72] and that $P_Z(n,t)$ can be found by means of the equation

$$\frac{d}{dt}P_Z(n,t)=\sum_{Z',n'}\lambda(Z,n|Z',n')[P_{Z'}(n',t)-P_Z(n,t)], \tag{25}$$

where $\lambda(Z,n|Z',n')$ is the microscopic transition probability $[\lambda(Z,n|Z',n')=\lambda(Z',n'|Z,n)]$.

The following treatment can be done in two ways. The first is associated with the introduction of a transition probability $\lambda(Z|Z')$ averaged over the set of transitions between the states n and n' of macroscopic cells[63] characterized by the values of the charge asymmetry Z and Z' and of the total energy in the interval from E to $E+\Delta E$:

$$\lambda(Z|Z')=N_Z^{-1}(E,E+\Delta E)N_{Z'}^{-1}(E,E+\Delta E)\times\sum_{n\in Z;E,E+\Delta E}\ \sum_{n'\in Z';E,E+\Delta E}\lambda(Z,n|Z',n'), \tag{26}$$

where $N_Z(E,E+\Delta E)\equiv\rho_Z(E)\Delta E$ is the number of states in the macroscopic cell, and $\rho_Z(E)$ is the density of states. This leads to the results formulated in Refs. 62 and 63.

The second way is associated with direct consideration of Eq. (25) without the introduction of averaged transition probabilities (26). This is possible by virtue of the relatively simple form of the Hamiltonian (5). As we shall see, such a treatment leads to the result obtained in Refs. 99 and 101 by a different method. The resulting expressions will serve as the basis for our further analysis.

We first consider the calculation of $\lambda(Z|Z')$. The microscopic transition probabilities can be expressed as follows in terms of the Hamiltonian (5):

$$\lambda(Z,n|Z',n')=\frac{1}{\Delta t}\left|\left\langle Z,n\right|T\times\exp\left(-\frac{i}{\hbar}\int_t^{t+\Delta t}\hat{\mathscr{H}}(\tau)d\tau\right)\left|Z',n'\right\rangle\right|^2, \tag{27}$$

where $|Z,n\rangle$ is the state vector of the system. The characteristic time Δt must exceed the relaxation time of the mean field of the nucleus (10^{-22} s) but must be less than $2\pi\hbar/\Delta E$, where ΔE is the energy spread of the states belonging to one macroscopic cell. Under the assumption that $\hat{V}_{\text{int}}$ is small compared with $\hat{H}_{\text{in}}$, we obtain

$$\lambda(Z,n|Z',n')=\frac{1}{\Delta t}|\langle Z,n|\hat{V}_{\text{int}}|Z',n'\rangle|^2\frac{\sin^2\frac{\Delta t}{2\hbar}(E_n^Z-E_{n'}^{Z'})}{(E_n^Z-E_{n'}^{Z'})^2/4}\equiv\frac{2\pi}{\hbar}|\langle Z,n|\hat{V}_{\text{int}}|Z',n'\rangle|^2\bar{\delta}^{(2\pi\hbar/\Delta t)}(E_n^Z-E_{n'}^{Z'}), \tag{28}$$

where the E_n^Z are determined by the equation

$$\hat{H}_{\text{in}}|Z,n\rangle=E_n^Z|Z,n\rangle.$$

The function $\bar{\delta}^{(2\pi\hbar/\Delta t)}(E_n^Z-E_{n'}^{Z'})$ is a macroscopic δ function. It is effectively equal to zero if n and n' belong to different macroscopic cells and is finite if n and n' belong to the same cell. We substitute (28) in (26):

$$\begin{aligned}\lambda(Z|Z')&=\frac{2\pi}{\hbar}N_Z^{-1}N_{Z'}^{-1}\sum_{n,n'}\sum_{k\neq k'}\langle Z,n|V_{kk'}|Z',n'\rangle\times\langle Z',n'|V_{kk'}^+|Z,n\rangle\bar{\delta}(E_n^Z-E_{n'}^Z)\\&=\frac{2\pi}{\hbar}N_Z^{-1}N_{Z'}^{-1}\sum_{k\neq k'}\sum_{n,n'}\langle Z,n|V_{kk'}\bar{\delta}(\hat{H}_{\text{in}}-E_n^Z)|Z',n'\rangle\langle Z',n'|V_{kk'}^+|Z,n\rangle\\&=\frac{2\pi}{\hbar}N_Z^{-1}N_{Z'}^{-1}\sum_{k\neq k'}\sum_{n}\sum_{Z'',\lambda}\langle Z,n|V_{kk'}\bar{\delta}(\hat{H}_{\text{in}}-E_n^Z)|Z'',\lambda\rangle\langle Z'',\lambda|V_{kk'}^+|Z,n\rangle.\end{aligned} \tag{29}$$

In the last expression, the index λ ranges over all macroscopic cells. The transition from a summation over n' to a summation over Z'' has become possible, first, because for fixed values of the indices k and k' only the one term with $Z''=Z'$ contributes to the sum over Z'' and, second, because the summation over n' can be extended to all macroscopic cells by virtue of the presence of the δ function $\bar{\delta}(\hat{H}_{\text{in}}-E_n^Z)$.

Using the completeness condition

$$\sum_{Z'',\lambda}|Z'',\lambda\rangle\langle Z'',\lambda|=1,$$

we obtain

$$\lambda(Z|Z')=\frac{2\pi}{\hbar}N_Z^{-1}N_{Z'}^{-1}\sum_{k\neq k'}\sum_{n}\langle Z,n|V_{kk'}\bar{\delta}(\hat{H}_{\text{in}}-E_n^Z)V_{kk'}^+|Z,n\rangle. \tag{30}$$

By means of the technique developed in Ref. 118, we obtained for the expression on the right-hand side of (30) the result[63]

$$\sum_n\langle Z,n|V_{kk'}\bar{\delta}(\hat{H}_{\text{in}}-E_n^Z)V_{kk'}^+|Z,n\rangle=\mu_0\rho_Z(E)\times\langle V_{kk'}V_{kk'}^+\rangle. \tag{31}$$

Here μ_0 is of order unity. The averaging in $\langle V_{kk'}V_{kk'}^+\rangle$ includes all shell configurations with given charge asymmetry Z.

Similarly, for the intermediate state in (29) we can use $|Z,n\rangle$. Then after symmetrization the expression (30) takes the form

$$\lambda(Z|Z')=\frac{2\pi}{\hbar}\frac{1}{(\Delta E)^2}\frac{1}{\sqrt{\rho_Z(E)\rho_{Z'}(E)}}\sum_{k\neq k'}\langle V_{kk'}V_{kk'}^+\rangle. \tag{32}$$

The averaged matrix element $\langle V_{kk'}V^{+}_{kk'}\rangle$ does not contain any traces of shell structure. Shell effects can enter (32) only through the experimental binding energies of the nuclei, on which the density of states ρ_Z of the system depends. The expression (32) is analogous to the expression for $\lambda_{ZZ'}$, in Ref. 62, in which a phenomenological approach was used:

$$\lambda_{ZZ'}=\frac{\lambda_0}{\sqrt{\rho_Z(E)\rho_{Z'}(E)}}.$$

The value of λ_0 was determined by the geometrical size of the dinuclear system.

We now return to Eqs. (25) and (28). For the configurations n and n', we can take states with fixed numbers of particles and holes. It follows from the single-particle nature of the interaction $\hat{V}_{\text{int}}$ that $\lambda(Z,n|Z',n')$ is nonzero only if the states n and n' differ by one particle–hole pair. The energy difference of the configuration in this case reduces to the difference of the single-particle energies. It follows from (28) that $Z'=Z\pm 1$. Substituting the expression for $\hat{V}_{\text{int}}$ in (28), we obtain

$$\lambda(Z,n|Z+1,n')=\frac{2\pi}{\hbar}\sum_{P,T}|g_{PT}|^2 n_P^{Z+1,n'}\times(1-n_T^{Z+1,n'})n_T^{Z,n}(1-n_P^{Z,n})\bar{\delta}(\varepsilon_P^Z-\varepsilon_T^Z),$$

$$\lambda(Z,n|Z-1,n')=\frac{2\pi}{\hbar}\sum_{P,T}|g_{PT}|^2 n_T^{Z-1,n'}\times(1-n_P^{Z-1,n'})n_P^{Z,n}(1-n_T^{Z,n})\bar{\delta}(\varepsilon_P^Z-\varepsilon_T^Z). \tag{33}$$

In (33), n_P and n_T are equal to zero or unity. Since the Hamiltonian is a single-particle operator, for fixed n' we have

$$\sum_n n_{T,P}^{Z,n}(1-n_{P,T}^{Z,n})=1. \tag{34}$$

We represent $P_Z(n',t)$ in the form

$$P_Z(n',t)\equiv P_Z(t)\Phi_Z(n'),$$

where $\Sigma_{n'}\Phi_Z(n')=1$. Here, $\Phi_Z(n')$ is the probability of finding the system for given charge asymmetry Z in the state n'. Such a representation corresponds to the assumption that the time required for establishment of an equilibrium distribution between the states belonging to one macroscopic cell is much shorter than the time of transition from one macroscopic cell to another. This assumption is always valid in transport theories, as we said in the Introduction.

We consider the sum

$$\sum_{n'} n_{P,T}^{Z,n'}(1-n_{T,P}^{Z,n'})\Phi_Z(n'). \tag{35}$$

In this expression, the product $n_{P,T}^{Z,n'}(1-n_{T,P}^{Z,n'})$ is averaged over all shell configurations belonging to the same macroscopic cell with given excitation energy. We assume that the sum (35) can be expressed by means of the thermal (Fermi) occupation numbers

$$\sum_{n'} n_{P,T}^{Z,n'}(1-n_{T,P}^{Z,n'})\Phi_Z(n')=N_{P,T}^{Z,n'}(T)(1-n_{T,P}^{Z,n'}(T)), \tag{35a}$$

where the temperature T is related to the excitation energy that characterizes the macroscopic cell. Substituting the relations (33–35) in (25), we obtain

$$\dot{P}_Z(t)=\Delta_{Z+1}^{(-)}P_{Z+1}(t)+\Delta_{Z-1}^{(+)}P_{Z-1}(t)-(\Delta_Z^{(-)}+\Delta_Z^{(+)})P_Z(t), \tag{36}$$

where

$$\Delta_z^{(+)}=\frac{1}{\Delta t}\sum_{P,T}|g_{PT}(R)|^2 n_T^Z(T)\times(1-n_P^Z(T))\frac{\sin^2\left(\frac{\Delta t}{2\hbar}[\tilde{\varepsilon}_P^Z-\tilde{\varepsilon}_T^Z]\right)}{(\tilde{\varepsilon}_P^Z-\tilde{\varepsilon}_T^Z)^2/4},$$

$$\Delta_Z^{(-)}=\frac{1}{\Delta t}\sum_{P,T}|g_{PT}(R)|^2 n_P^Z(T)\times(1-n_T^Z(T))\frac{\sin^2\left(\frac{\Delta t}{2\hbar}[\tilde{\varepsilon}_P^Z-\tilde{\varepsilon}_T^Z]\right)}{(\tilde{\varepsilon}_P^Z-\tilde{\varepsilon}_T^Z)^2/4}. \tag{37}$$

The single-particle spectrum and the degeneracies of the levels occur directly in the calculations of the transition probabilities $\Delta_Z^{(\pm)}$. Thus, the $\Delta_Z^{(\pm)}$ reflect the influence of the shell effects on the evolution of the system. In contrast to (32), the expression (37) does not contain explicitly the total densities of states of the system for given charge asymmetry and total energy. They appeared in (32) as a result of configuration averaging of the transition matrix element. Because of the configuration averaging, (32) also has no dependence of the matrix elements of the interaction Hamiltonian on the quantum numbers of the single-particle states. Of course, the densities of the single-particle states are actually included in the calculations in accordance with the expressions (37) through the details of the shell structure.

Allowance for the mutual influence of the mean fields of the nuclei in (5) leads to a change of the difference of the single-particle energies[100,101] in (37):

$$\varepsilon_P-\varepsilon_T\to\tilde{\varepsilon}_P-\tilde{\varepsilon}_T=\varepsilon_P-\varepsilon_T+\frac{(Z_T-Z_P)e^2}{2R},$$

where $Z_{P,T}$ are the charges of the nuclei of the dinuclear system. Because of its long-range nature, the Coulomb interaction makes the main contribution to the shift in the energies of the proton single-particle levels. In highly asymmetric configurations, the proton levels in the light fragment are appreciably shifted upward in energy relative to the single-particle levels of the heavy fragment, i.e., the Fermi surface of the light fragment is higher than in the heavy one. This fact is indirectly confirmed in experiments on transfer reactions. When the projectile ion is much lighter than the target

nucleus, the measured cross sections for proton stripping from the light nucleus are much greater than the cross sections for neutron stripping.[5]

Results of calculations of charge distributions

We calculated the charge distributions of the products of the ^{52}Cr(378 MeV)+^{181}Ta, ^{51}V(447 MeV)+^{197}Au, and ^{20}Ne(175 MeV)+^{197}Au reactions. In the calculation of the transition probabilities (37), we used realistic single-particle level schemes. The scale of the single-particle energies was fixed in such a way that the energy of the last occupied level corresponded to the experimental nucleon separation energy.[119] To simplify the numerical calculations, the matrix elements g_{PT} were parametrized[3,63,64] as follows:

$$g_{PT}=g_0\exp\left(-\frac{|\tilde{\varepsilon}_P-\tilde{\varepsilon}_T|}{\Delta}\right)\exp\left(-\frac{|j_P-j_T|}{\Delta j}\right)\delta_{m_P m_T}, \tag{38}$$

where $\Delta=8$–10 MeV, $\Delta_j=6$–9, and

$$g_0=\int d\mathbf{r}\left(\frac{\rho_P^Z(\mathbf{r})}{Z_P}\right)^{1/2}\frac{1}{2}\left(U_P^Z(\mathbf{r})+U_T^Z(\mathbf{r})\right)\left(\frac{\rho_T^Z(\dot{\mathbf{r}})}{Z_T}\right)^{1/2}.$$

Here, ρ_P^Z and ρ_T^Z are the proton densities of the nuclei used to parametrize the radial wave functions. The value of Δt was taken to be 10^{-22} s.

The results of the calculation of the transition probabilities $\Delta_Z^{(\pm)}$ for the ^{52}Cr+^{181}Ta reaction are given in Fig. 13 for two values of the temperature, $T=0.5$ MeV and $T=2.0$ MeV, corresponding to a larger and smaller impact parameter for given energy of the projectile. The oscillatory nature of the dependence of $\Delta_Z^{(\pm)}$ on Z reflects the influence of the shell structure. The probabilities $\Delta_Z^{(\pm)}$ have local minima at $Z=2$ and 8, corresponding to magic nuclei. The absence of local minima of $\Delta_Z^{(\pm)}$ for the other magic numbers may be due to the structure of the conjugate fragments and the influence of the neutron system. The stability of a system with charge asymmetry Z' is determined not only by the local minima of $\Delta_Z^{(\pm)}$ but also by the condition $\Delta_Z^{(+)}>\Delta_Z^{(-)}$ for $Z<Z'$ and $\Delta_Z^{(+)}<\Delta_Z^{(-)}$ for $Z>Z'$. Such a condition is satisfied for $Z'=40$ (the conjugate fragment has $N=82$) and around $Z'=48$ (the system is close to a symmetric configuration and to $Z=50$).

With increasing temperature of the system, the influence of the shell effects on the process of nucleon transfer decreases. This is reflected in a certain decrease with increasing temperature of the oscillations of $\Delta_Z^{(\pm)}$ with varying Z (Fig. 13). The transition probabilities $\Delta_Z^{(\pm)}$ depend on the temperature only through the Fermi occupation numbers (37). As an example, we analyze the T dependence of $(\Delta_Z^{(-)}-\Delta_{Z+1}^{(-)})$:

$$s\Delta_Z^{(-)}-\Delta_{Z+1}^{(-)}=\sum_{P,T}F_{PT}(n_P^Z(T)(1-n_T^Z(T))-n_P^{Z+1}(T)(1-n_T^{Z+1}(T))), \tag{39}$$

where F_{PT} denotes the product of quantities that do not depend on the temperature. In (39) we have ignored the change of the single-particle energies on the transition $Z\to Z+1$.

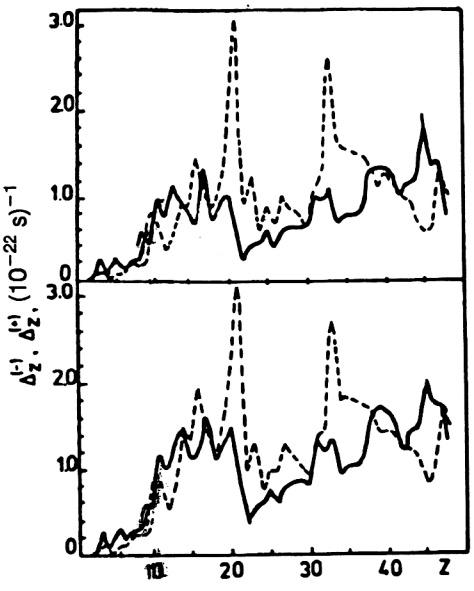

FIG. 13. Transition probabilities $\Delta_Z^{(\pm)}$ for the ^{52}Cr+^{181}Ta reaction calculated for two temperatures. The upper part of the figure is for $T=0.5$ MeV and the lower part is for $T=2.0$ MeV. The solid continuous curve is for $\Delta_Z^{(-)}$, and the dashed curve is for $\Delta_Z^{(+)}$.

In the case of highly asymmetric configurations, the separation between the single-particle levels in the light fragment is greater than the temperature T in the considered region of excitation energies, i.e., the deviation of $n_P^Z(T)$ from 1 or 0 is small, and the shell effects are manifested more clearly. For nearly symmetric configurations, the change in the fragment Fermi energies $\Delta\varepsilon_{F_P,F_T}$ on the transition $Z\to Z+1$ is less than T, and therefore the expression in the brackets in (39) can be written approximately as

$$n_P^Z(1-n_T^Z)-n_P^{Z+1}(1-n_T^{Z+1})\approx\frac{1}{T}n_P^Z(1-n_T^Z)[n_T^Z\Delta\varepsilon_{F_T}-(1-n_P^Z)\Delta\varepsilon_{F_P}].$$

In the sum (39) the main contribution is made by the terms with $n_T^Z(T)\approx n_P^Z(T)$, i.e.,

$$\Delta_Z^{(-)}-\Delta_{Z+1}^{(-)}\sim\frac{\Delta\varepsilon_{F_T}}{T}. \tag{40}$$

It can be concluded from (40) that the weakening of the influence of the shell structure on the process of nucleon transfer with increasing T takes place more slowly than the exponential decrease of the shell correction to the binding energy of the nuclei.[120] Similar conclusions follow from consideration of the difference $(\Delta_Z^{(+)}-\Delta_{Z+1}^{(+)})$.

The results of the calculations of P_Z for the ^{52}Cr(379 MeV)+^{181}Ta reaction corresponding to different interaction times and temperatures are given in Figs. 14 and 15. In Fig. 14, the calculated dependence of P_Z was obtained for interaction time $t_{\text{int}}=10^{-21}$ s and $T=1.5$ MeV. In this case, the comparison is made with the experimental data on σ_Z of Ref. 17, which are characteristic of the products of deep inelastic transfers. It can be seen from Fig. 14 that inclusion of the Coulomb interaction improves the agreement between the

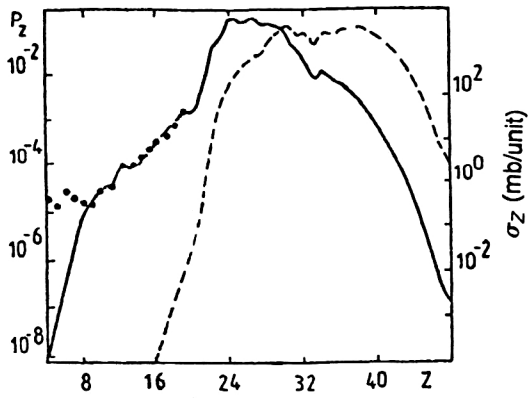

FIG. 14. Charge distribution of the products of deep inelastic transfers for the ^{52}Cr(378 MeV)+^{181}Ta reaction. The results of the calculation of P_Z for $t_{int}=10^{-21}$ s and $T=1.5$ MeV with and without allowance for the Coulomb interaction are shown by the solid continuous and dashed curves, respectively. The black circles are the experimental values of the cross sections σ_Z from Ref. 17.

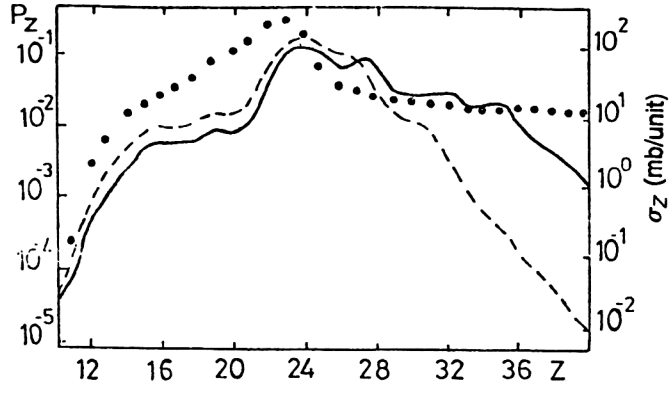

FIG. 16. Charge distribution P_Z of products of the ^{51}V(447 MeV)+^{197}Au reaction calculated for $t_{int}=10^{-21}$ s, $T=2.0$ MeV with allowance (solid continuous curve) and without allowance (dashed curve) for N/Z equilibrium. The experimental values of the cross sections σ_Z from Ref. 122 are shown by the black circles.

theoretical results and the experimental data. It can also be seen that the Coulomb interaction increases the probability of formation of light nuclei. The large difference between the theoretical and experimental results for $Z<8$ is probably due to the higher probability of decay of the dinuclear system in the case of large charge asymmetry for dynamical reasons. The experimental data on the multiplicity of γ rays[121] show that for $Z\leqslant 8$ collisions with $l<l_{crit}$ make an important contribution to the product production cross section, i.e., there exists an additional mechanism of production of light products that is not taken into account in our calculations.

In the same reaction, measurements were also made of the charge distributions of the products, which are characterized by an angular distribution that is symmetric in the center-of-mass system. These experimental data[17] are compared in Fig. 15 with the theoretical results obtained for an interaction time $t_{int}=5\cdot 10^{-21}$ s, which is longer than in Fig. 14, and $T=2.0$ MeV, corresponding to collisions with $l \approx l_{B_f=0}$ (the maximum angular momentum at which fusion is still possible). It can be seen that there is qualitative agreement between the theoretical and experimental results. For comparison, Fig. 15 also shows the results of our calculation in the liquid-drop approximation.[62] It can be seen that by taking into account shell effects it is possible to explain the cross sections for production of light nuclei. The results presented above were obtained under the assumption that N/Z equilibrium in the system is established before the commencement of nucleon exchange.

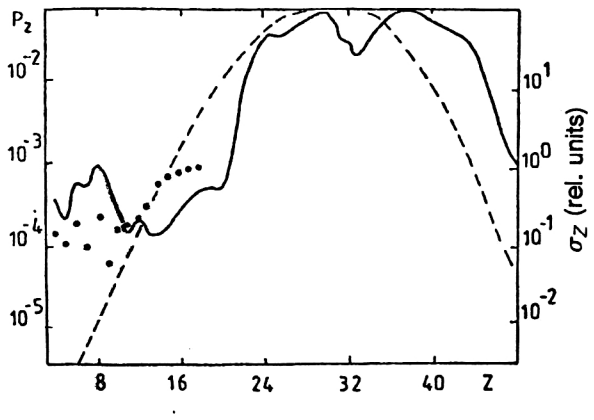

FIG. 15. Charge distribution of products having an angular distribution symmetric in the center-of-mass system for the ^{52}Cr(378 MeV)+^{181}Ta reaction. The solid continuous curve is the calculated value of P_Z for $t_{int}=5\cdot 10^{-21}$ s and $T=2.0$ MeV. The dashed curve shows P_Z obtained in accordance with the model of Ref. 62. The black circles give the experimental values of the cross sections σ_Z from Ref. 17.

The theoretical results together with the experimental data for the ^{51}V(447 MeV)+^{197}Au reaction are shown in Fig. 16. The experimental charge distribution[122] is integrated over the angles in the center-of-mass system and over the final kinetic energy ($20°\leqslant\theta_{cm}\leqslant 90°$, $100\leqslant E\leqslant 340$ MeV). Therefore, quasielastic processes are taken into account in the experimental cross sections σ_Z for $Z\approx 23$. This is probably the reason for the discrepancy between the theoretical and experimental data near $Z=23$. The broad plateau of the charge distribution for large Z evidently corresponds to quasifission processes.

In Fig. 16 we give for comparison the theoretical charge distribution obtained without allowance for establishment of N/Z equilibrium, i.e., the N/Z ratio in the light fragment was taken to be equal to the N/Z ratio in the projectile. We see that there is a large difference between the theoretical and experimental results at large Z. Therefore, the question of the establishment of N/Z equilibrium is important for the theoretical analysis of the charge distribution of the reaction products of many-nucleon transfers.

Satisfactory qualitative agreement was also obtained for the charge distribution of the products of deep inelastic transfers in the ^{20}Ne(175 MeV)+^{197}Au reaction.[123] The results given in Fig. 17 were obtained for $t_{int}=10^{-21}$ s and $T=1.0$ MeV.

The theoretical results reproduce fairly well the structure of the charge distributions. For large values of the charge asymmetry, the difference between the energy shifts of the single-particle states of the light and heavy fragments due to

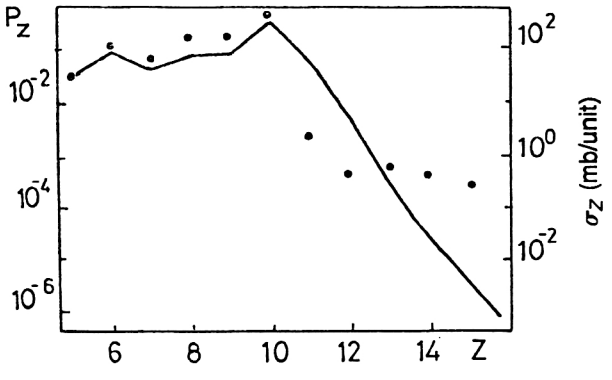

FIG. 17. Charge distribution of products of deep inelastic transfers for the ^{20}Ne(175 MeV)+^{197}Au reaction. The solid continuous curve gives the calculation of P_Z for $t_{int}=10^{-21}$ s, $T=1.0$ MeV. The black circles give the experimental values of the cross sections σ_Z from Ref. 123.

the Coulomb interaction reaches the greatest value. This leads to a significant enhancement in the yields of light nuclei. The results of the calculations of the charge distributions were found to be sensitive to the isotopic composition of the interacting fragments, and therefore the problem of the establishment of N/Z equilibrium in the system is important for study of many-nucleon transfer reactions.

Microscopic treatment of proton and neutron transfers in deep inelastic heavy-ion collisions

Strictly speaking, the treatment of nucleon transfer in the microscopic approach requires consideration of transfers of both protons and neutrons, since shell effects (closed shells, the appearance near the Fermi surface of a level with high degeneracy) are manifested in the transfers of both protons and neutrons. This makes the results of a calculation sensitive to the assumption of the establishment of N/Z equilibrium in the system.[52,96–101] In the previous subsection, the number of neutrons in the light fragments was specified using the condition of their β stability and the establishment of N/Z equilibrium in the system, i.e., it was assumed that on the transfer of one proton the corresponding number of neutrons is transferred practically instantaneously. This assumption was a limitation of the theory and made it impossible to take into account shell effects associated with neutrons.

The interest in a microscopic treatment of proton and neutron transfers is also due to the problem of describing the establishment of N/Z equilibrium between colliding nuclei.[7] Study of the charge and mass distributions in reactions with light nuclei such as ^{40}Ar+^{42,48}Ca and ^{40}Ar+^{50}Ti (Ref. 124) showed that even at small kinetic-energy losses, i.e., for short interaction times, the N/Z ratio for the reaction products is equal to the N/Z ratio for the compound system. In this case, exchange of a pair of nucleons already leads to the attainment of N/Z equilibrium. For heavy interacting nuclei, the process of establishment of N/Z equilibrium is more prolonged. It is possible that this process takes place through the presence of either a collective isovector mode or independent exchange of particles. In the latter case, the relaxation of the N/Z ratio has a stochastic nature. Consideration of this process in the framework of the microscopic model makes it possible to obtain arguments for or against this point of view.

The formulation of the microscopic method for describing the charge and mass distributions becomes particularly topical in connection with the development of radioactive beams and the planned production and investigation of exotic nuclei. Calculations can help in choosing the initial combination of colliding nuclei needed to obtain the maximum yields of the isotopes of interest.

For the simultaneous treatment of proton and neutron transfers in the dinuclear system, the mean single-particle potentials $U_{P,T}$ in (5) include both the nuclear and the Coulomb (for the protons) fields and can be represented in the form[125]

$$U^Z_{P,T}(\mathbf{r})=U_{0_{P,T}}(\mathbf{r})-\frac{N_{P,T}-Z_{P,T}}{4A_{P,T}}V_1(\mathbf{r})+U_{C_{P,T}}(\mathbf{r}),$$

$$U^N_{P,T}(\mathbf{r})=U_{0_{P,T}}(\mathbf{r})+\frac{N_{P,T}-Z_{P,T}}{4A_{P,T}}V_1(\mathbf{r}). \tag{41}$$

Here Z_P and Z_T are the charges of the fragments, N_P and N_T are the numbers of neutrons in them, and $A_{P,T}=Z_{P,T}+N_{P,T}$ are the mass numbers. The second term in the expressions (41) is the isovector correction (symmetry potential) for the average nuclear potential, and $U_{C_{P,T}}$ is the Coulomb potential of the corresponding fragment. For the nuclear part of the single-particle potential (41) we can, for example, use the parametrization[126]

$$U_{0_{P,T}}(\mathbf{r})\pm\frac{N_{P,T}-Z_{P,T}}{4A_{P,T}}V_1(\mathbf{r})$$
$$=-\frac{V_0(1\pm\gamma(N_{P,T}-Z_{P,T})/A_{P,T})}{1+\exp[(r-R_{0_{P,T}})/a]}, \tag{42}$$

where $V_0=53.3$ MeV, $\gamma=0.63$, $a=0.63$ fm, and $R_{0_{P,T}}=1.24\cdot A^{1/3}_{P,T}$ fm. As in the calculations of the charge distributions, we shall not take into account the nondiagonal matrix elements $\chi_{PP'}$ and $\chi_{TT'}$. It is assumed that their influence can be taken into account by the introduction of temperature-dependent occupation numbers of the single-particle levels.

As in the case of (36), we can obtain equations for the probabilities $P_{Z,N}(t)$ for finding the system at the time t in a state in which the light fragment has charge Z and neutron number N:

$$\dot{P}_{Z,N}(t)=\Delta^{(-,0)}_{Z+1,N}P_{Z+1,N}(t)+\Delta^{(+,0)}_{Z-1,N}P_{Z-1,N}(t)$$
$$+\Delta^{(0,-)}_{Z,N+1}P_{Z,N+1}+\Delta^{(0,+)}_{Z,N-1}P_{Z,N-1}(t)-(\Delta^{(-,0)}_{Z,N}$$
$$+\Delta^{(+,0)}_{Z,N}+\Delta^{(0,-)}_{Z,N}+\Delta^{(0,+)}_{Z,N})P_{Z,N}(t) \tag{43}$$

with transport coefficients

$$\Delta^{(\pm,0)}_{Z,N}=\frac{1}{\Delta t}\sum_{P,T}|g^Z_{PT}(R)|^2n^Z_{T,P}(T)$$
$$\times(1-n^Z_{P,T}(T))\frac{\sin^2\left(\frac{\Delta t}{2\hbar}[\tilde{\varepsilon}^Z_P-\tilde{\varepsilon}^Z_T]\right)}{(\tilde{\varepsilon}^Z_P-\tilde{\varepsilon}^Z_T)^2/4},$$

$$\Delta_{Z,N}^{(0,\pm)}=\frac{1}{\Delta t}\sum_{P,T}|g_{PT}^{N}(R)|^2 n_{T,P}^{N}(T)$$

$$\times(1-n_{P,T}^{N}(T))\,\frac{\sin^2\left(\frac{\Delta t}{2\hbar}[\bar{\varepsilon}_P^N-\bar{\varepsilon}_T^N]\right)}{(\bar{\varepsilon}_P^N-\bar{\varepsilon}_T^N)^2/4}. \qquad (44)$$

The values of the matrix elements and the single-particle energies are determined in accordance with (6).

The symmetry forces together with the Coulomb interaction are responsible for the relative difference of the characteristic times of proton and neutron transfer and the establishment of N/Z equilibrium in the system. The direction of nucleon transfer will be determined by the relative positions of the Fermi surfaces in the interacting nuclei.

Charge and mass distributions

On the basis of the proposed model, we investigated the charge and mass distributions of the products of the following reactions: ^{238}U+^{40}Ca (340 MeV), ^{238}U+^{48}Ca (425 MeV), ^{197}Au+^{40}Ar (292 MeV), and ^{100}Mo+^{40}Ar (270 MeV). The first two of them are of interest for study of the influence of the symmetry forces. In the ^{238}U+^{40}Ca reaction, the ratios N/Z in the colliding nuclei differ strongly, and therefore there is a large surface gradient of the potential energy. In contrast, in the ^{238}U+^{48}Ca case the ratios N/Z are already close to the equilibrium value for the compound system, i.e., the system has a small surface gradient of the potential energy near the initial point of evolution. The final reaction is interesting because it has been observed to have a large mass dispersion despite a small change in the mass number of the light fragment.

To calculate the transport coefficients (44), we use realistic schemes of single-particle levels, and we parametrize the matrix elements g_{PT} in accordance with (38). We have not calculated the cross sections for the yields of isotopes for each partial wave but considered some average trajectory, the most probable one for the given collision. The interaction time can be determined as in Ref. 62. Because there is little evaporation of protons from the reaction products, the interaction time was corrected using the experimental values of the charge variances.

To illustrate the possibilities of the model for describing the evolution of dinuclear systems, Fig. 18 shows the theoretical and experimental[8,9] charge distributions of the products of the reactions ^{238}U+^{40}Ca (340 MeV) and ^{238}U+^{48}Ca (425 MeV). The calculated curves were obtained for interaction time $t_{\text{int}}=2\cdot10^{-21}$ s and $T=1.5$ MeV, this being characteristic of deep inelastic transfer reactions. The theoretical results agree qualitatively with the experimental ones. The larger than calculated yield of light particles may be due to the contribution of collisions with $l<l_{\text{crit}}$ and the increase in the probability of decay of strongly asymmetric systems (Refs. 17, 78, 106, and 127–129).

Figure 19 gives for these reactions the dependence on the kinetic-energy loss (E_{loss}) of the mean values of the mass, $\langle A\rangle$, charge number, $\langle Z\rangle$, and neutron number, $\langle N\rangle$, of the light fragment. The experimental data are well described by the proposed model at small E_{loss}. At large E_{loss}, there is a

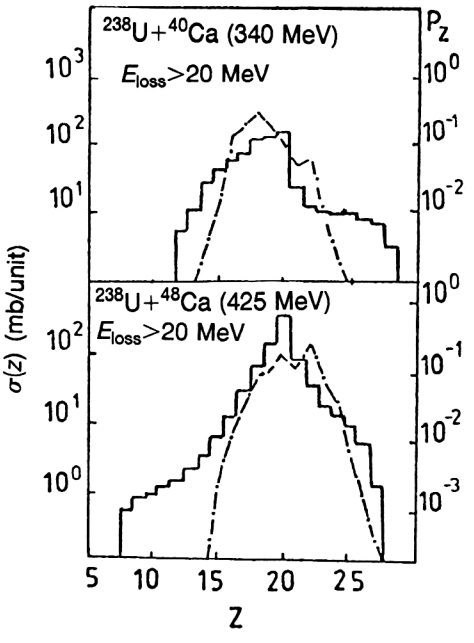

FIG. 18. Charge distributions P_Z of products of the ^{238}U+^{40}Ca (340 MeV) and ^{238}U+^{48}Ca (425 MeV) reactions calculated for $t_{\text{int}}=2\cdot10^{-21}$ s and $T=1.5$ MeV (dot–dash curves). The solid continuous curves show the experimental values of the cross sections σ_Z from Refs. 8 and 9.

deviation of the calculated values from the experimental ones. We note that the theoretical curves were obtained without allowance for nucleon evaporation. In our view, inclusion of this process would improve the agreement with experiment, as in Refs. 8 and 9. However, the difference between the calculated and experimental values of $\langle Z\rangle$ at large E_{loss}—the difference reaches two units for ^{238}U+^{40}Ca reactions—cannot be explained solely by proton-evaporation processes. The difference may be due[10] to pre-equilibrium effects in the first stage of the reaction, the contribution of collective charge transfer through excitation of giant isovector resonances, and α-cluster transfer.[45,46]

As was shown in Sec. 2, the establishment of thermal equilibrium in the dinuclear system does not occur instantaneously. The direction of the correction in the calculated dependences due to the contribution of pre-equilibrium processes can be determined in calculations made without the assumption of the establishment of thermal equilibrium in the system, for example, in the case of equality of the excitation energies of the interacting nuclei. Such a calculation was made for the ^{238}U+^{48}Ca reaction (Fig. 19). The deviation of these results from the ordinary dependences obtained under the condition of complete thermal equilibrium in the dinuclear system is most pronounced at large E_{loss} and leads to better agreement with the experimental data.

To illustrate the role of the symmetry forces in the processes of many-nucleon transfers, Fig. 19 (dashed curve) shows the result of a calculation for the ^{238}U+^{48}Ca reaction made without inclusion of the isovector part of the single-particle potential. This reaction was chosen because of the large difference of the N/Z ratios in the colliding nuclei. It can be clearly seen that allowance for the symmetry forces improves the agreement with the experimental data. The best

agreement between the theory and experiment in the $^{238}U+^{48}Ca$ reaction for the values of $\langle Z\rangle$ can be achieved if the isovector part g_{PT} is increased by a factor 2, but we did not find a theoretical justification for this. It is possible that agreement with the experimental data will be improved if instead of the parametrization (38) for g_{PT} we use the exact expression (see the Appendix). However, this requires a large volume of calculations.

Good agreement of the theoretical and experimental dependences of the second moments of the Z, N, and A distributions on E_{loss} was obtained for the $^{238}U+^{40}Ca$ and $^{238}U+^{48}Ca$ reactions (Fig. 20).

Satisfactory agreement between the theoretical and experimental results is obtained when one considers the dependences of σ_A^2/σ_Z^2 and $\langle A\rangle/\langle Z\rangle$ on E_{loss} for the $^{238}U+^{40,48}Ca$ reactions (Fig. 21). It can be seen that at small energy losses the ratio σ_A^2/σ_Z^2 is close to $\langle A\rangle/\langle Z\rangle$, and, as is well known,[7] this means that in the initial stage of the reaction proton exchange is dominant. With increase of the interaction time (increase of E_{loss}), the ratio σ_A^2/σ_Z^2 becomes close to $(\langle A\rangle/\langle Z\rangle)^2$, and this also corresponds to a strong correlation between the proton and neutron transfers. Analyzing the dependences in Fig. 21, we may conclude that the establishment of N/Z equilibrium is a monotonic continuous process.

It was established experimentally[1,5] that the cross sections for production of the isotopes of light products ($Z\leqslant 8$) in deep inelastic reactions satisfy the Q_{gg} systematics. The apparent violation of the Q_{gg} systematics at $Z>8$ is due to

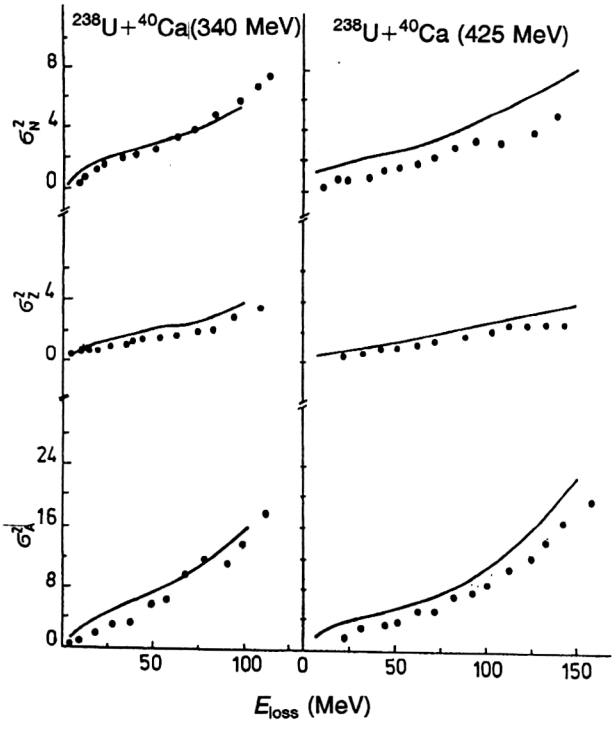

FIG. 20. Mass (σ_A^2) and charge (σ_Z^2) variances, and variance (σ_N^2) of the neutron number, shown as functions of the kinetic-energy loss for the $^{238}U+^{40,48}Ca$ reactions. The black circles show the experimental data of Refs. 8 and 9, and the curves are the results of the calculations.

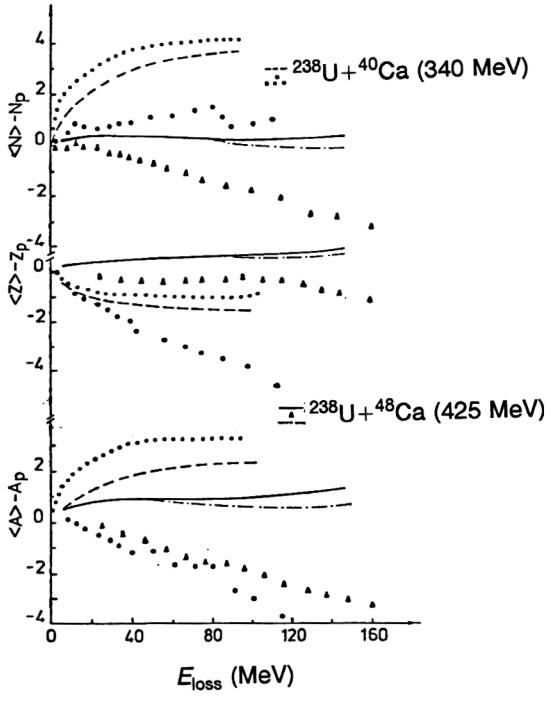

FIG. 19. Deviations of the mean values of the mass, $\langle A\rangle$, charge, $\langle Z\rangle$, and neutron number, $\langle N\rangle$, from the initial values as functions of the energy loss in the $^{238}U+^{40,48}Ca$ reactions. The experimental data of Refs. 8 and 9 are shown by the black circles and triangles. The results of the calculation are shown by the solid continuous curve ($^{238}U+^{40}Ca$) and dashed curve ($^{238}U+^{48}Ca$), respectively. The results obtained without allowance for symmetry forces are shown by the dotted curves. The dot–dash curve shows the results obtained without the assumption of thermal equilibrium.

the influence of secondary nuclear processes—evaporation of nucleons and α particles from the excited light fragment. To justify the use of the Q_{gg} systematics, static arguments, which are manifestly not applicable in our model, are usually employed.[130] It is therefore not obvious in advance that our results reproduce the experimentally observed Q_{gg} systematics. Calculations of P_{ZN} ($t_{\text{int}}=3\cdot10^{-21}$ s and $T=1.5$ MeV) for the $^{197}Au+^{40}Ar$ (292 MeV) reaction showed (Fig. 22) that the ratio of isotope yields characteristic of the Q_{gg} systematics with allowance for corrections for nonpairing of the

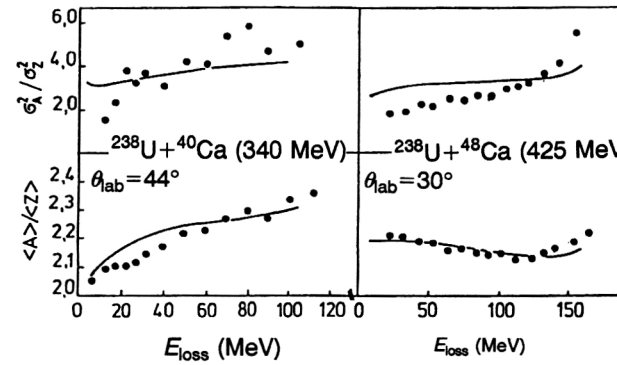

FIG. 21. Dependence of $\langle A\rangle/\langle Z\rangle$ (lower part) and σ_A^2/σ_Z^2 (upper part) on the kinetic-energy loss for the $^{238}U+^{40,48}Ca$ reactions. The black circles are the experimental data of Refs. 8 and 9. The results of the calculations are shown by the curves.

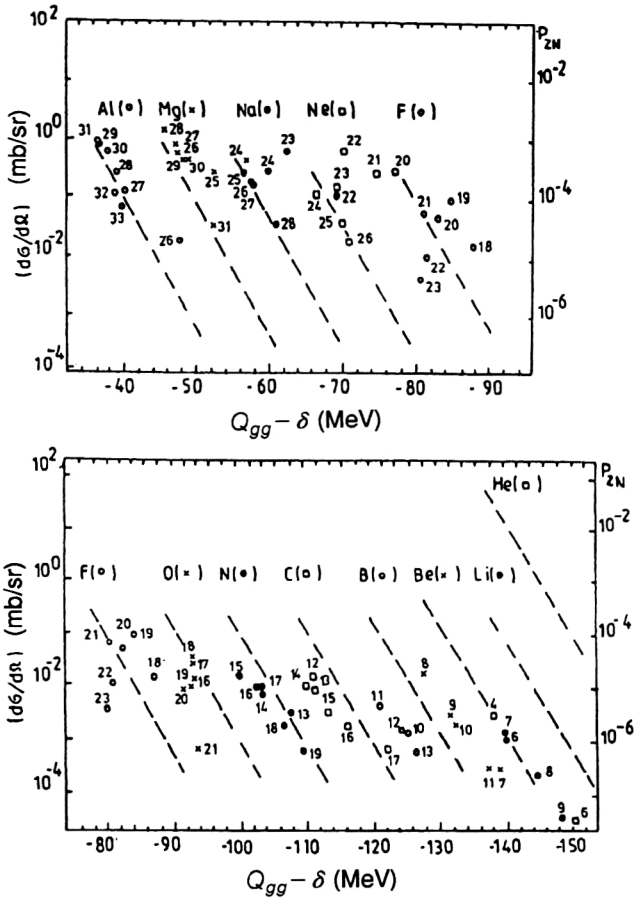

FIG. 22. Cross sections for production of isotopes as functions of $(Q_{gg}-\delta)$ for the ^{197}Au+^{40}Ar (292 MeV) reaction. The dashed lines correspond to the approximation of the experimental data of Ref. 1. The results of the calculation of P_{ZN} are shown by the symbols ($t_{int}=3\cdot10^{-21}$ s). The numbers next to the symbols are the mass numbers of the isotopes.

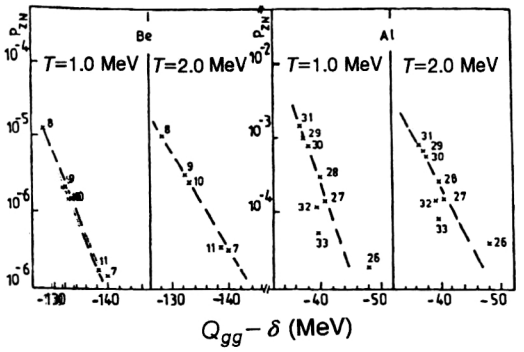

FIG. 23. Cross sections for production of Al and Be isotopes as functions of $(Q_{gg}-\delta)$, calculated for two values of the temperature, $T=1.0$ and 2.0 MeV ($t_{int}=3\cdot10^{-21}$ s) (crosses), for the ^{197}Au+^{40}Ar (292 MeV) reaction. The numbers next to the symbols are the mass numbers of the isotopes. The dashed lines are the results of approximation of the calculated data.

nucleons on their transfer from the donor to the acceptor nucleus is reproduced by the model for $Z\geqslant11$ (except for ^{24}Mg and ^{22,23}Na) and $Z<8$. The dashed lines in Fig. 22 correspond to the experimental values. A possible reason for the discrepancy between the calculated absolute yields of the light particles and the experimental yields was noted in the discussion of Fig. 18. In our view, the disagreement of the calculations for the O, F, and Ne isotopes with the Q_{gg} systematics could be due to the fact that in our model we do not consider cluster transfer, which may be important for these nuclei. For example, for the isotopes ^{24}Mg and $^{20-22}$Ne the α-particle separation energy is close to or even less than the nucleon separation energy. Therefore, allowance for cluster transfer could reduce the calculated yields of certain light isotopes and improve the agreement with the Q_{gg} systematics. In addition, cluster transfer will make an additional contribution to the production of products with $Z<8$.

In accordance with the Q_{gg} systematics, the cross sections for production of isotopes can be represented in the form[5]

$$\sigma\propto\exp[(Q_{gg}-\delta+\Delta E_C)/T_0], \qquad (45)$$

where ΔE_C is the change in the Coulomb energy of the system due to proton transfer, and δ is the correction for the nonpairing of the nucleons on their transfer. The parameter T_0 differs from the ordinary thermodynamic temperature T, i.e., the slope of the lines in the Q_{gg} systematics characterizes T only through the functional dependence of T_0 and T. Calculation of the Q_{gg} systematics for Al and Be for $T=1.0$ and 2.0 MeV and for the same interaction time (Fig. 23) showed that the slope of the lines decreases with increasing T, i.e., the dependence (45) is reproduced qualitatively. However, the slope changes by less than a factor 2, confirming the inequivalence of T_0 and T.

As we have already noted, standard transport calculations that use only the potential-energy surface do not always correctly describe the evolution of the dinuclear system. For example, by means of these models it is not possible to explain the large dispersions of the mass distribution for a small change of $\langle A\rangle$ for the ^{100}Mo+^{40}Ar (270 MeV) reaction.[13,78] The fact is that the evolution of the system is influenced not only by the relative positions of the Fermi surfaces of the protons and neutrons in the interacting nuclei but also by the details of the shell structure of the fragments (the number of free and occupied levels near the Fermi surface, the degree of their degeneracy, etc.). The first effect is taken into account by the "driving" potential. However, the others can be included in the treatment only on the basis of a microscopic model. Our model, which takes into account explicitly the effects of the shell structure for the protons and neutrons, makes it possible to describe the experimental results well (Fig. 24).

Calculation of the yields of isotopes of heavy products of incomplete-fusion reactions

As an application of the microscopic model of nucleon transfer, we consider the method of calculating the yields of neutron-rich nuclei in incomplete-fusion reactions.[131] As follows from the results of Sec. 2, the excitation energy of the heavy reaction product may be low. Therefore, the number of particles that evaporate from it is small. Such reactions have been intensively studied[132,133] in order to use them to obtain neutron-rich actinides. The calculation of the cross sections

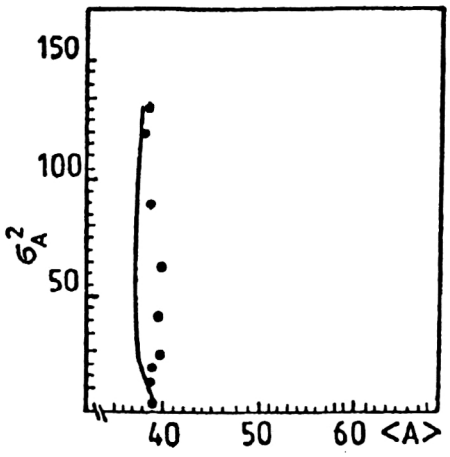

FIG. 24. Dependence of the mass variance σ_A^2 on the mean value $\langle A \rangle$ of the light-fragment mass number for the ^{100}Mo+^{40}Ar (270 MeV) reaction. The black circles show the experimental data of Ref. 78. The curve shows the results of the calculation.

for the yields of different nuclei in the reaction consists of two stages. In the first, the pre-evaporation distribution of the reaction products is calculated. Then, using this distribution, one calculates the yield of the evaporation particles and obtains the final distribution of nuclei, which is compared with the experimental data.

Solving Eqs. (43), we can obtain the pre-evaporation distribution of the reaction products. The calculated cross sections for the production of isotopes are in agreement with the Q_{gg} systematics. Using the parametrization (45), it is easy to determine T_0, which characterizes the slope of the dependence of P_{ZN} on a logarithmic scale for given Z. The results of the calculation for the ^{18}O(97 MeV)+^{248}Cm reaction are shown in Fig. 25. By calculating the yields of the isotopes of several nuclei and determining T_0, one can then also find the pre-evaporation yield of other nuclei.

Reactions in which a large number of nucleons of the projectile nucleus is transferred to the target nucleus ($A_P + A_T \rightarrow A_P' + A_T'$) are called incomplete-fusion reactions. In

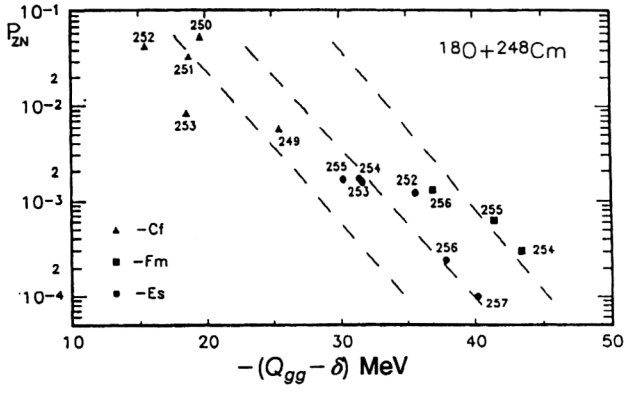

FIG. 25. Calculated values of P_{ZN} as a function of Q_{gg} for the ^{18}O(97 MeV)+^{248}Cm reaction (shown by the black symbols). The results of approximation in accordance with the expression (45) are shown by the dashed lines.

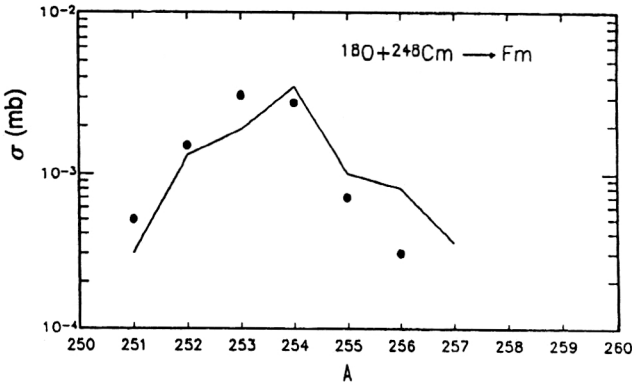

FIG. 26. Calculated cross sections for production of Fm isotopes (continuous line). The experimental data of Ref. 137 are shown by the black circles.

accordance with the model of Ref. 134, the cross section for channel i (A_P' and A_T' are given) of incomplete fusion has the form

$$\sigma(i) = \pi\lambda^2 \sum_{l=0}^{l_{\max}} (2l+1) \times T_l \frac{P_l^i \exp[(Q_{gg}^i - \delta + \Delta E_C)/T_0]}{\Sigma_i P_l^i \exp[(Q_{gg}^i - \delta + \Delta E_C)/T_0]}, \quad (46)$$

where $P_l^i = \{1+\exp[(l-l_{\text{lim}}(i))/\Delta]\}^{-1}$, and T_l is the penetrability of the entrance potential barrier for the lth partial wave. The limiting angular momentum for the ith channel is determined by

$$l_{\text{lim}}(i) = \frac{A_P}{A_P - A_P'} l_{\text{crit}}(A_T + (A_P - A_P')),$$

where $l_{\text{crit}}[A_T + (A_P - A_P')]$ is the critical angular momentum in the channel $[A_T + (A_P - A_P')]$.[132] The summation in (36) is up to $l_{\max}$, at which the nuclei in the collision can still reach the region of attraction of the nucleus–nucleus potential. The parameter Δ is usually taken to be a few units of $\hbar$. At a collision energy only slightly greater than the entrance potential barrier, the dependence of the parameter T_0 on l can be ignored.

The process of deexcitation of the heavy fragment was considered in the framework of the statistical approach of Refs. 135 and 136, which is based on the Monte Carlo method. Since the reaction products have relatively large spin, one can use the semiclassical approximation, in which the spins of the evaporated particles are ignored and all the angular momenta are regarded as classical vectors. The energy spectrum of the reaction products exhibits the presence of both a deep inelastic and a quasielastic component. The widths and relative contributions of these components are parameters of the model. The evaporation model takes into account the emission of photons, neutrons, protons, ^{2}H, ^{3}H, ^{3}He, ^{4}He and fission. For realistic values of the parameters, good agreement between the theoretical and experimental cross sections for the yields of the Fm isotopes in the ^{18}O(97 MeV)+^{248}Cm reaction was obtained (Fig. 26).[137]

We conclude this section with a summary. We have investigated the transfer of protons and neutrons in deep inelastic heavy-ion collisions in the framework of a microscopic model. The calculated reaction characteristics exhibit good agreement with the experimental data. We have established that the isospin dependence of the single-particle potential is important for the description of the experimental data. The calculated cross sections for production of isotopes of light elements were found to be in agreement with the Q_{gg} systematics. It was noted that the excess of the experimental over the calculated yield of light particles could be due to the increase in the probability of decay of highly asymmetric systems for dynamical reasons.

4. MICROSCOPIC "DRIVING" POTENTIAL

Connection between the driving potential and the transport coefficients

For the description of the evolution of dinuclear systems, wide use is made of transport models, in which the change in the probability $P_Z(t)$ for finding the dinuclear system at the time t in a state with charge asymmetry Z can be described by the master equation (36). The transport coefficients $\Delta_Z^{(\pm)}$ characterize the probability of transitions of a proton from the heavy nucleus to the light one ($\Delta_Z^{(+)}$) and vice versa ($\Delta_Z^{(-)}$). The neutron transfer is described similarly (see Sec. 3). The right-hand side of Eq. (36) takes into account only the transitions $Z \rightleftarrows Z+1$ and $Z \rightleftarrows Z-1$, as in the independent-particle model. In Sec. 3, the transport coefficients were obtained in the framework of the microscopic model of deep inelastic heavy-ion collisions of Refs. 52 and 96–101.

The time independence of the transport coefficients of Eq. (36) and the form of the coefficient of $P_Z(t)$ guarantee the existence of a steady solution of the master equation. Equating the left-hand side of (36) to zero, we obtain the time-independent conditions

$$\begin{aligned} \Delta_{Z-1}^{(+)} P_{Z-1} &= \Delta_Z^{(-)} P_Z , \\ \Delta_{Z+1}^{(-)} P_{Z+1} &= \Delta_Z^{(+)} P_Z . \end{aligned} \tag{47}$$

Both expressions in (47) are equivalent to the relation

$$\frac{P_{Z+1}}{P_Z} = \frac{\Delta_Z^{(+)}}{\Delta_{Z+1}^{(-)}} . \tag{48}$$

As $t \to \infty$, the probability $P_Z(t)$ tends to its steady limit, which is proportional to the level density. For fixed total energy of the dinuclear system, the level density ρ_Z is proportional to $\exp\{-\tilde{U}(Z)/T\}$.[62] Here, $\tilde{U}(Z)$ is the ground-state energy of the dinuclear system with charge asymmetry Z. The thermodynamic temperature T can be expressed in terms of the excitation energy E_J^* of the system in the framework of the Fermi-gas approximation: $T = (E_J^*/a)^{1/2}$, where $a = (A_P + A_T)/8$ MeV, in which A_P and A_T are the mass numbers of the light and heavy fragments, respectively. The excitation energy E_J^* depends on the kinetic energy and on the collision orbital angular momentum of the projectile ion.

Using Eq. (48) and the fact that $P_Z(t)$ is proportional to the level density ρ_Z, we obtain the following relation for the transport coefficients:

$$\frac{\Delta_{Z+1}^{(-)}}{\Delta_Z^{(+)}} = \exp\left[\frac{\tilde{U}(Z+1) - \tilde{U}(Z)}{T}\right]. \tag{49}$$

This expression makes it possible to establish an iterative procedure for the recovery of $\tilde{U}(Z)$:

$$\tilde{U}(Z+1) = \tilde{U}(Z) + T \ln\left(\frac{\Delta_{Z+1}^{(-)}}{\Delta_Z^{(+)}}\right). \tag{50}$$

Using (50) and the values of the transport coefficients, we can calculate $\tilde{U}(Z)$ for any Z. It should be noted that the expression (50) was obtained directly from the master equation (36) without additional assumptions about the form of the transport coefficients $\Delta_Z^{(\pm)}$. Thus, the realistic determination of $\Delta_Z^{(\pm)}$ enables us to consider the behavior of $\tilde{U}(Z)$. In accordance with (49), the ground-state energy $\tilde{U}(Z)$, as a function of the light-fragment charge Z, completely determines the direction of evolution of the dinuclear system, which depends on the position of the entrance point relative to the Businaro–Gallone point. In macroscopic models, $\tilde{U}(Z)$ is called the driving potential.

Microscopic and phenomenological driving potentials

There are two ways of calculating $\Delta_Z^{(\pm)}$: macroscopic and microscopic. In phenomenological models[62] describing many-nucleon transfers, one uses a parametrization of the transport coefficients $\Delta_Z^{(\pm)}$ in which $\tilde{U}(Z)$ is equated to the potential energy $U(Z)$ of the dinuclear system calculated as the sum of the binding energies of the nuclei and the nucleus–nucleus potential. In principle, $\tilde{U}(Z)$ and $U(Z)$ need not be equal, since $\tilde{U}(Z)$ includes the kinetic energy as well as the potential energy. For example, because of the quantum nature of the dinuclear system, $\tilde{U}(Z)$ contains the energy of the zero-point vibrations. However, the difference should not be large and the main features in the behavior of $\tilde{U}(Z)$ and $U(Z)$ must be the same, since the phenomenological model gives a qualitatively correct description of the behavior of many reactions. From our point of view, the given comparison can be one of the ways of testing our method of calculating the transport coefficients in Eq. (36).

In Ref. 62, the difference between $U(Z)$ and $\tilde{U}(Z)$ was ignored, and for the transport coefficients the following parametrization was proposed:

$$\Delta_Z^{(\pm)} = s_0 \exp\{[U(Z) - U(Z \pm 1)]/2T\}, \tag{51}$$

where s_0 is a constant that characterizes the time scale. This parametrization is a direct consequence of the expression (49).

The parametrization (51) is based on macroscopic characteristics of the system. In the phenomenological models, the potential energy of the system is taken in the form of a sum of the liquid-drop energy of the fragments, a shell correction, whose contribution decreases with increasing excitation energy of the system, and the potential energy of the nucleus–nucleus interaction:

$$U(Z)=U_{LD}(Z)+U_{SH}(Z)\exp(-E_J^*/E_0)+U_{\text{int}}(Z,R). \tag{52}$$

The parameter E_0 characterizes the exponential damping of the shell correction with increasing E_J^*. The potential of the nucleus–nucleus interaction $U_{\text{int}}(Z,R)$ includes the Coulomb and nuclear potentials. The nuclear part can be taken in the well-known form of the "proximity" potential. For heavy systems and small J, the rotational energy is ignored.[138]

The $\Delta_Z^{(\pm)}$ dependence of the macroscopic transition probabilities $P_Z(t)$ is determined under the assumption that on the transfer of nucleons from one fragment to the other the dinuclear system can go over to any state allowed by the energy conservation law. In such a treatment, shell effects enter $U(Z)$ only through the binding energies, without explicit allowance for the structure of the single-particle spectrum of the interacting nuclei, although its influence is confirmed by the various experimental facts mentioned in the Introduction. Therefore, for the analysis of these shell effects a microscopic model must be used.

In the microscopic model of Refs. 99–101 (see Sec. 3) the details of the structure of the interacting nuclei are explicitly taken into account in the microscopically calculated transport coefficients $\Delta_Z^{(\pm)}$ (37) and influence the evolution of the dinuclear system. Allowance for the shell structure significantly restricts the probability of transition of a nucleon by virtue of the effect of the selection rules with respect to the projection of the single-particle angular momentum and the spin. Near the Fermi surfaces of the interacting nuclei there may be single-particle levels between which transitions are weakened by the weak overlap of the single-particle wave functions. This indicates richer possibilities for describing the dynamics of dinuclear systems in the microscopic approach.

Let us consider the connection between the relation (48) and the particular form of the transport coefficients (37). For short times Δt we have approximately

$$\frac{\Delta_{Z+1}^{(-)}}{\Delta_Z^{(+)}}=\frac{\Sigma_{P,T}|g_{PT}|^2 n_P^{Z+1}(T)(1-n_T^{Z+1}(T))}{\Sigma_{P,T}|g_{PT}|^2 n_T^{Z}(T)(1-n_P^{Z}(T))}. \tag{53}$$

In Ref. 99, thermal occupation numbers were introduced by averaging over the configurations n' of the macroscopic state of a dinuclear system with given Z. Therefore, in place of (53) we can write

$$\frac{\Delta_{Z+1}^{(-)}}{\Delta_Z^{(+)}}=\frac{\Sigma_{n'}\Sigma_{P,T}\Phi_{Z+1}(n')|g_{PT}|^2 n_P^{Z+1,n'}(1-n_T^{Z+1,n'})}{\Sigma_{n'}\Sigma_{P,T}\Phi_{Z}(n')|g_{PT}|^2 n_T^{Z,n'}(1-n_P^{Z,n'})}, \tag{54}$$

where $\Phi_Z(n')$ is defined in (35). In (54), $n_P^{Z,n'}$ and $n_T^{Z,n'}$ are equal to zero or unity, since n' characterizes a configuration with a given number of particles and holes. We can write approximately

$$\Phi_Z(n')\approx\frac{1}{N_Z},$$

where $N_Z\equiv\rho_Z\Delta E$ is the number of states in the macroscopic subsystem. Substituting this expression in (54), we obtain

$$\frac{\Delta_{Z+1}^{(-)}}{\Delta_Z^{(+)}}\cong\frac{\rho_Z}{\rho_{Z+1}}\frac{\Sigma_{n'}\Sigma_{P,T}|g_{PT}|^2 n_P^{Z+1,n'}(1-n_T^{Z+1,n'})}{\Sigma_{n'}\Sigma_{P,T}|g_{PT}|^2 n_T^{Z,n'}(1-n_P^{Z,n'})}$$

or, using the explicit expression for the microscopic transfer matrix elements (54),

$$\frac{\Delta_{Z+1}^{(-)}}{\Delta_Z^{(+)}}\cong\frac{\rho_Z}{\rho_{Z+1}}\frac{\Sigma_{n'}\lambda(Z,n|Z+1,n')}{\Sigma_{n'}\lambda(Z+1,n|Z,n')}. \tag{55}$$

Because of the single-particle nature of the interaction in the Hamiltonian of the dinuclear system, there is a one-to-one correspondence between n and n'. Therefore, we can replace the sum over n' in the denominator of the expression (55) by a sum over n. Since $\lambda(Z+1,n|Z,n')=\lambda(Z,n|Z+1,n')$, we finally obtain the relation

$$\frac{\Delta_{Z+1}^{(-)}}{\Delta_Z^{(+)}}\cong\frac{\rho_Z}{\rho_{Z+1}},$$

which is none other than (49). Thus, in our microscopic approach we have obtained the same relations between the transport coefficients as in the phenomenological model.

Results of calculations

We compare the microscopically calculated potential $\tilde{U}(Z)$ with the macroscopic potential $U(Z)$ used in phenomenological models. As an example, we consider a dinuclear system with $Z_{\text{tot}}=108$, which is realized in the ^{40}Ar (220 MeV)+^{239}Th and ^{32}S(192 MeV)+^{238}U reactions, which lead to similar compound nuclei with the same excitation energy ($E_J^*=34$ MeV) but possessing qualitatively different charge (mass) distributions of the reaction products.[14,139]

To calculate the transport coefficients $\Delta_Z^{(\pm)}$ (37), we take the matrix elements $g_{PT}(R)$ from Ref. 102, in which a relatively simple analytic method for calculating them, valid for appreciable overlaps of the nuclear densities, was proposed and realized. For a separation between the centers of the nuclei satisfying $R\geqslant R_{\varepsilon_P}+R_{\varepsilon_T}$ [$R_{\varepsilon_{P(T)}}$ is the radius of matching the wave functions inside and outside the nucleus for the given single-particle state $P(T)$], they have the form

$$g_{PT}(R)=(-1)^{l_T+m_T+1/2}C_{l_T}^{\text{ex}}C_{l_P}^{\text{ex}}\sqrt{(2j_P+1)(2j_T+1)}$$
$$\times\sum_L\left(j_T-\frac{1}{2},j_P\,\frac{1}{2}\middle|L0\right)(j_T-m_T,j_Pm_P|L0)$$
$$\times[A_Pk_L(\nu_PR)+A_Tk_L(\nu_TR)]. \tag{56}$$

For $R<R_{\varepsilon_P}+R_{\varepsilon_T}$, a different expression is used:

$$g_{PT}(R)=(-1)^{l_T+m_T+1/2}C_{l_T}^{\text{ex}}C_{l_P}^{\text{ex}}\sqrt{(2j_P+1)(2j_T+1)}$$
$$\times\sum_L j_T-\frac{1}{2},j_P\,\frac{1}{2}\,|L0)(j_T-m_T,j_Pm_P|L0)$$
$$\times\{(-1)^{(L-l_T-l_P)/2}[B_Py_L(\kappa_PR)+B_Ty_L(\kappa_TR)$$
$$+D_Pj_L(\kappa_PR)+D_Tj_L(\kappa_TR)]+G_Pk_L(\nu_PR)$$
$$+G_Tk_L(\nu_TR)+I_{PT}^0(R,L)\}. \tag{57}$$

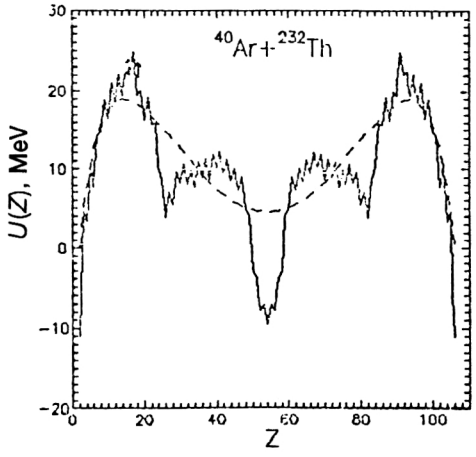

FIG. 27. Phenomenological "driving" potential $\tilde{U}(Z)$ for the system with $Z_{tot}=108$ and $A_{tot}=272$ for $T=0$ MeV. The results obtained in the framework of the liquid-drop model are shown by the dashed curve. The driving potential calculated using the experimental binding energies of the nuclei in (52) are shown by the continuous curve.

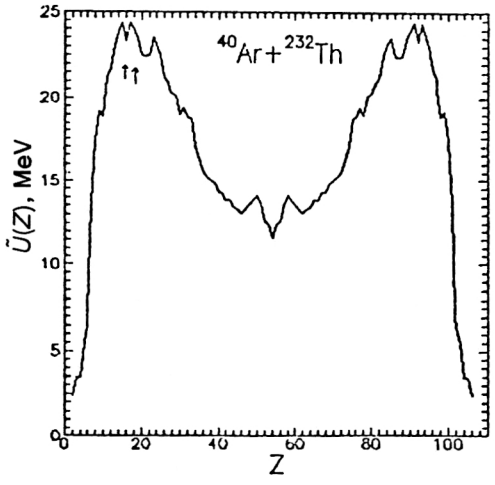

FIG. 28. Microscopic driving potential calculated for the system with $Z_{tot}=108$ and $A_{tot}=272$ ($T=1.0$ MeV and $R=R_P+R_T$). The arrows indicate the initial systems ^{32}S+^{238}U and ^{40}Ar+^{232}Th.

Here $j_L(x)$, $i_L(x)$, $k_L(x)$, and $y_L(x)$ are spherical Bessel functions (Ref. 140), $l_{P(T)}$ and $j_{P(T)}$ are the orbital and total single-particle angular momenta, respectively, and $m_{P(T)}$ is the projection of the angular momentum $j_{P(T)}$. The expressions for the normalization coefficients $C^{ex}_{P(T)}$, the constants $A_{P(T)}$, $B_{P(T)}$, $D_{P(T)}$, $G_{P(T)}$, which depend on the quantum numbers of the single-particle states, and the quantities $I^0_{PT}(R,L)$ are given in the Appendix. The wave numbers for the exterior and interior parts of the wave functions are determined as follows:

$$\nu_{P(T)}=\sqrt{\frac{2m}{\hbar^2}\{B_{coul}-\varepsilon_{P(T)}\}},$$

$$\kappa_{P(T)}=\sqrt{\frac{2m}{\hbar^2}\{\varepsilon_{P(T)}-\tilde{U}_{P(T)}\}},$$

where $\tilde{U}_{P(T)}$ is the mean potential of the light (heavy) nucleus in the single-particle state P (T), m is the proton mass, and B_{coul} is the Coulomb barrier of the nucleus.

The results of the calculations of the phenomenological and microscopic potentials [the expressions (52), (50), and (37), respectively] for the dinuclear system with $Z_{tot}=108$ are given in Figs. 27 and 28. We assume that N/Z equilibrium is established in the system in the initial stage of the reaction. The isotopic composition for elements with $Z<10$ is taken from data on the Q_{gg} systematics of the cross sections for production of isotopes in the analogous reactions.[1,5] The dependence of the microscopic driving potential on the angular momentum is taken into account through the temperature parameter T of the dinuclear system.

It can be seen that the microscopic and macroscopic potentials are qualitatively similar. They have certain characteristic maxima and minima, reflecting the influence of the shell structure on the evolution of the dinuclear system. The absence of local minima in $\tilde{U}(Z)$ for certain magic and even values of Z can be explained by the shell structure of the conjugate fragment and the influence of the neutron subsystem. It should be noted that, compared with the phenomenological potential, the microscopic potential $\tilde{U}(Z)$ is more sensitive to the isotopic composition of the fragments, this being reflected especially in the greater width of the Businaro–Gallone maximum with increasing ratio N/Z in the light fragment. To illustrate this, Fig. 29 shows the microscopically calculated driving potential for the ^{63}Cu+^{197}Au reaction, in which $Z_{tot}=108$ and $A_{tot}-260$, i.e., the system has a smaller number of neutrons than in the preceding cases.

At the same time, the microscopic potential $\tilde{U}(Z)$ is less sensitive to an increase in the temperature T of the dinuclear system. This is reflected in the weak decrease in the depth of the local minima, whereas the depth of the local minima of the phenomenological potential increases strongly with increasing T. Since $\Delta^{(\pm)}_Z-\Delta^{(\pm)}_{Z+1}\sim 1/T$ (Ref. 100) [see (40)] for almost symmetric configurations of the dinuclear system, the weakening of the influence of the shell structure on the process of nucleon transfer with increasing temperature T is slower than the exponential decrease of the shell correction to the liquid-drop binding energy of the nuclei. When speak-

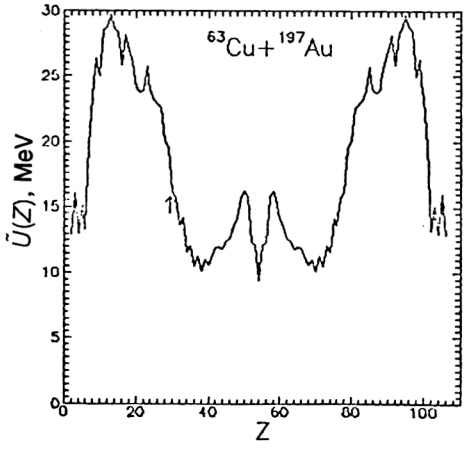

FIG. 29. The same as in Fig. 28 but for the system with $Z_{tot}=108$ and $A_{tot}=260$ ($T=1.0$ MeV and $R=R_P+R_T$). The arrow shows the position of the initial ^{63}Cu+^{197}Au configuration.

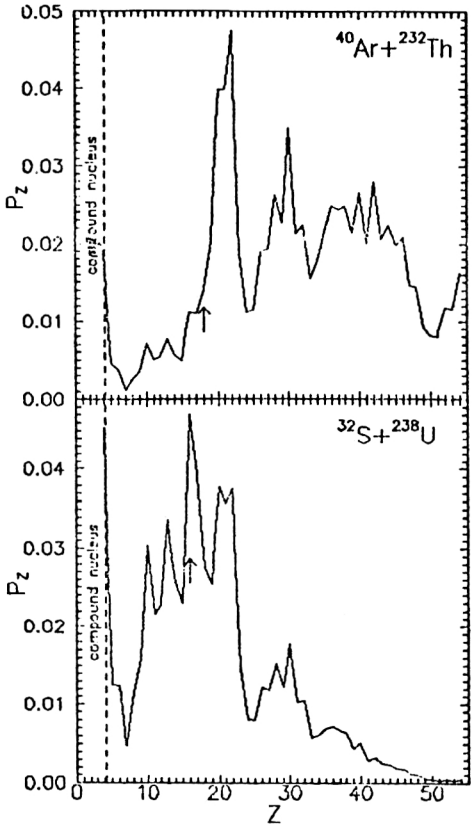

FIG. 30. Charge distributions calculated for the reactions $^{40}Ar+^{232}Th$ ($T=1.0$ MeV, $R=R_P+R_T$, and $t=4\cdot10^{-21}$ s) and $^{32}S+^{238}U$ ($T=1.0$ MeV, $R=R_P+R_T$, and $t=3\cdot10^{-21}$ s).

ing of shell effects in the microscopic treatment, we have in mind the influence of the single-particle spectra near the Fermi surfaces of the interacting nuclei on the process of nucleon exchange. This approach is based on the idea that the nuclei of the dinuclear system retain their individuality (Refs. 1, 5, 6, and 16).

The charge distributions of the products of the $^{40}Ar+^{232}Th$ and $^{32}S+^{238}U$ reactions (Fig. 30), calculated by means of the macroscopic transport coefficients, agree qualitatively with the experimental data of Refs. 14 and 139. There is a qualitatively correct description of the direction of evolution of the system, the maxima in the yields of the reaction products, and the relationship between the fusion and quasifission channels. This last fact is readily determined if one regards the fusion process as motion of the dinuclear system in the direction of increasing mass asymmetry, and quasifission[16] as decay of the dinuclear system into a nearly symmetric configuration. For the $^{32}S+^{238}U$ reaction, more than 50% of the cross section corresponds to the fusion channel, whereas for the $^{40}Ar+^{232}Th$ reaction only 20% does. Accordingly, the remaining contribution to the cross section comes from the quasifission channel. Such a strong change in the product yields as a function of the charge (mass) asymmetry of the entrance channel can be explained by the difference between the structures of the interacting nuclei. Since the single-particle spectra near the Fermi surfaces of the nuclei ^{232}Th and ^{238}U differ little, the evolution of the dinuclear system is mainly affected by the structure of the light partner. Namely, in the nucleus ^{32}S the first unoccupied proton levels are far removed from the Fermi surface, and this significantly reduces the probability of proton transfer from the heavy fragment. In the nucleus ^{40}Ar, conversely, there is an unoccupied proton level with high degeneracy near the Fermi surface. This leads to a decrease in the matter symmetry of the dinuclear system. The charge distribution P_Z has a maximum around $Z=20$, corresponding to a magic light nucleus. The N/Z ratio of the system influences the ratio of the cross sections for fusion and quasifission in the reaction. For the $^{63}Cu+^{197}Au$ reaction, approximately 15% of the cross section corresponds to an increase of the mass symmetry, in good agreement with the experimental results.[141]

Thus, in the framework of the microscopic approach it is possible to obtain qualitative agreement between the results of the calculations of the charge distributions and the experimental data. The phenomenological and microscopic approaches use different input data. Nevertheless, the results of the calculations exhibit a remarkable similarity of the microscopic and phenomenological potentials. This can serve as a further confirmation of the validity of the microscopic model, which is based on the concept that the nuclei retain their individuality. Allowance for the selection rules for the angular momentum and its projection has the consequence that in the microscopic version we obtain a driving potential, which carries more information about the paths of evolution of the system. This potential was found to be more sensitive to a change in the isotopic composition of the parts of the dinuclear system.

CONCLUSIONS

For the description of the dynamics of deep inelastic heavy-ion collisions, microscopic models are widely used. Their use to explain the formation of the observed distributions of the reaction products with respect to the excitation energy, mass, and charge is fairly successful. This means that these microscopic models adequately reflect the nature of the considered processes. Knowledge of the distribution of the excitation energy between the fragments is needed to recover the initial yield of reaction products from the measured yields of evaporation remnants. The results show that the excitation energy at the time of collision of the two nuclei is distributed approximately equally between them and not in proportion to their masses. The influence of the shell structure of the interacting nuclei on this distribution is important. Nucleon exchange, especially neutron exchange, is the main mechanism of dissipation of the kinetic energy. However, for heavy systems the contribution to the dissipation from the particle–hole excitations becomes comparable with the contribution of the exchange mechanism.

The microscopic model based on a single-particle Hamiltonian with a time-dependent mean field makes it possible to take into account the influence of the shell structure of the interacting nuclei on the formation of the charge and mass distributions in many-nucleon transfer reactions and to investigate the evolution of dinuclear systems in a wide range of variation of the mass (charge) asymmetry. In this

approach, allowance for the Coulomb interaction of the parts of the dinuclear system reduces to a renormalization of the proton single-particle energies. This effect leads to an appreciable increase in the probability of formation of strongly asymmetric configurations of dinuclear systems, in which shell effects are manifested most strongly. With increasing excitation energy of the system, the influence of the shell structure on the process of nucleon transfer decreases more slowly than the shell correction to the binding energy of the nuclei.

For the consideration of the transfer of both protons and neutrons in deep inelastic heavy-ion collisions, it is necessary to take into account the isospin dependence of the single-particle potential in order to describe the experimental data. The calculated cross sections for production of elements agree with the Q_{gg} systematics. The microscopic calculation of the pre-evaporation yield of reaction products can be used, for example, to estimate the yields of neutron-rich actinides.

Analysis of the results of calculations of the charge and mass distributions makes it possible to propose the existence of not only nucleon but also cluster transfers in dinuclear systems. The calculations confirm the conclusions of the experimental studies that the process of establishment of N/Z equilibrium in heavy systems occurs throughout the interaction time. It should be noted that in the framework of the proposed model we have not been able to reproduce quantitatively the yields of light nuclei in deep inelastic heavy-ion collisions. The decay of a highly asymmetric dinuclear system probably occurs for dynamical reasons. Allowance for this factor could have a strong influence on the enhancement of the yields of light nuclei and improve the agreement with experiment. In some cases, the change of the charge asymmetry of the dinuclear system during the dissipation of the kinetic energy may be important.

A further confirmation of the large possibilities of the microscopic approach is the qualitative agreement between the microscopically calculated and phenomenological driving potentials. At the same time, the analysis shows that the microscopic driving potential carries more information about the paths of evolution of the dinuclear systems.

The further development of the model will, in our view, permit a self-consistent description of the dissipation of kinetic energy and the change of the mean field of the dinuclear system, and will make it possible to calculate the cross sections for production of the various reaction products with allowance for the probability of decay of each configuration of the dinuclear system.

We thank V. V. Volkov for numerous discussions throughout the entire period of work on our series of papers. We are also grateful to V. E. Bunakov, A. S. Il'inov, E. A. Cherepanov, and Yu. M. Chuvil'skiĭ for their great interest in the work and for valuable comments. This work was in part supported by the International Science Foundation (grant N RFJ000).

APPENDIX. CALCULATION OF NUCLEON-TRANSFER MATRIX ELEMENTS

We approximate the radial wave functions of the single-particle states by the wave functions of a finite-depth rectangular well $\bar{U}_i (i=P,T)$:

$$\psi_i(\mathbf{r}) = \psi_{l_i}(r) Y^{l_i 1/2}_{j_i m_i}(\mathbf{r}/r),$$

$$\psi_{l_i}(r) = \begin{cases} C^{\text{in}}_{l_i} j_{l_i}(\kappa_i r), & r \leqslant R_{\varepsilon_i} \\ C^{\text{ex}}_{l_i} k_i(\nu_i r), & r \geqslant R_{\varepsilon_i}, \end{cases}$$

$$Y^{l_i 1/2}_{j_i m_i} = \sum_{m\sigma} \left(l_i m, \frac{1}{2}\sigma \middle| j_i m_i \right) Y_{l_i m_i} \chi_\sigma , \qquad \text{(A1)}$$

where $Y^{l_i 1/2}_{j_i m_i}$ is a spherical harmonic, j_i is a spherical Bessel function of the first kind, and k_l is a spherical Macdonald function. In the case of heavy nuclei, the wave functions (A1) can be regarded as a fairly good approximation. In contrast to harmonic-oscillator wave functions, they have the correct asymptotic behavior, and analytic calculations using them are fairly simple. For the single-particle spectrum, we take the spectrum for a spherically symmetric Woods–Saxon potential U_i $(i=P,T)$ that contains central, spin–orbit, and Coulomb (for the protons) interactions. To the profile U_i we shall also "match" interior and exterior radial wave functions. Thus, for each single-particle state with energy ε_i we shall determine a corresponding matching radius R_{ε_i} by means of the relation $U_i(R_{\varepsilon_i}) = \varepsilon_i$. The wave functions for the protons and neutrons will be taken in the same form, but because of the difference of the single-particle potentials the matching radii will differ, and therefore the values of the wave functions for equal quantum numbers will also differ.

The normalization constants are found from the condition of continuity of the logarithmic derivative of the radial wave function and the normalization:

$$C^{\text{ex}}_{l_{P(T)}} = \sqrt{2} \left[R^3_{\varepsilon_{P(T)}} \left(1 + \frac{\nu^2_{P(T)}}{\kappa^2_{P(T)}} \right) \right.$$
$$\left. \times k_{l_{P(T)}+1}(\nu_{P(T)} R_{\varepsilon_{P(T)}}) k_{l_{P(T)}-1}(\nu_{P(T)} R_{\varepsilon_{P(T)}}) \right]^{-1/2}$$

$$C^{\text{in}}_{l_{P(T)}} = \frac{k_{l_{P(T)}}(\nu_{P(T)} R_{\varepsilon_{P(T)}})}{j_{l_{P(T)}}(\kappa_{P(T)} R_{\varepsilon_{P(T)}})} C^{\text{ex}}_{l_{P(T)}} . \qquad \text{(A2)}$$

In the coordinate representation, the matrix element for nucleon transfer has the form[8]

$$g_{PT}(R) = \tfrac{1}{2} \int d\mathbf{r} \psi^*_T(\mathbf{r}) [U_T(\mathbf{r}) + U_P(\mathbf{r}-\mathbf{R})] \psi_P(\mathbf{r}-\mathbf{R}), \qquad \text{(A3)}$$

where $[U_T(\mathbf{r}) + U_P(\mathbf{r}-\mathbf{R})]$ is the total single-particle potential of the dinuclear system, and R is the distance between the centers of the nuclei. Using the Fourier transforms of the wave functions

$$\psi_{P(T)}(\mathbf{p}) = \psi_{P(T)}(p) Y^{l_{P(T)} 1/2}_{j_{P(T)} m_{P(T)}}(\mathbf{p}/p),$$

$$\psi_{P(T)}(p)=i^{-l_{P(T)}}\sqrt{\frac{2}{\pi}}\,C^{\rm ex}_{l_{P(T)}}R^2_{\varepsilon_{P(T)}}\,\frac{\kappa^2_{P(T)}+\nu^2_{P(T)}}{(p^2+\nu^2_{P(T)})(\kappa^2_{P(T)}-p^2)}$$
$$\times[pk_{l_{P(T)}}(\nu_{P(T)}R_{\varepsilon_{P(T)}})j_{l_{P(T)}-1}(pR_{\varepsilon_{P(T)}})$$
$$+\nu_{P(T)}k_{l_{P(T)}-1}(\nu_{P(T)}R_{\varepsilon_{P(T)}})j_{l_{P(T)}}(pR_{\varepsilon_{P(T)}})],\quad\text{(A4)}$$

and the approximate relation

$$\left(-\frac{\hbar^2}{2m}\Delta+U_{P(T)}(\mathbf{r})\right)\psi_{P(T)}(\mathbf{r})=\varepsilon_{P(T)}\psi_{P(T)}(\mathbf{r}),$$

we obtain the following expression for the transfer matrix element:

$$g_{PT}(R)=\frac{1}{2}\int d\mathbf{p}e^{i\mathbf{pR}}\psi^*_T(\mathbf{p})\left[\left\{\varepsilon_P-\frac{\hbar^2}{2m}p^2\right\}+\left\{\varepsilon_T-\frac{\hbar^2}{2m}p^2\right\}\right]\psi_P(\mathbf{p}).\quad\text{(A5)}$$

Integrating (A5) over the angular variables, we obtain

$$g_{PT}(R)=\frac{(-1)^{m_T-1/2}}{2}\sqrt{(2j_P+1)(2j_T+1)}$$
$$\times\sum_L i^L(j_T-1/2,j_p1/2|L0)(j_T-m_T,j_Pm_p|L0)$$
$$\times\int_0^\infty dpp^2j_L(pR)\left[\left\{\varepsilon_P-\frac{\hbar^2p^2}{2m}\right\}+\left\{\varepsilon_T-\frac{\hbar^2p^2}{2m}\right\}\right]\psi_{l_T}(p)\psi_{l_P}(p).\quad\text{(A6)}$$

The integrand in (A6) is an analytic function and has simple poles at the points $p=\pm i\nu_{P(T)}$, $\pm\kappa_{P(T)}$. Using this circumstance, we obtain the final results.

For $R\geqslant R_{\varepsilon_P}+R_{\varepsilon_T}$, we obtain the expression (56), where

$$A_{P(T)}=a_{P(T)}\xi(i_{l_{T(P)}}(\nu_{P(T)}R_{\varepsilon_{T(P)}})),$$
$$a_{P(T)}=\frac{(\varepsilon_P+\varepsilon_T+h^2\nu^2_{P(T)}/m)(\nu^2_{T(P)}+\kappa^2_{T(P)})R^2_{\varepsilon_{P(T)}}}{2(\nu^2_{P(T)}+\kappa^2_{T(P)})(\nu^2_{P(T)}-\nu^2_{T(P)})},$$
$$\xi(f_{l_{P(T)}}(\kappa'R_{\varepsilon_{P(T)}}))=f^2_{l_{P(T)}}(\kappa'R_{\varepsilon_{P(T)}})\frac{\partial}{\partial R_{\varepsilon_{P(T)}}}\times\left(\frac{k_{l_{P(T)}}(\nu_{P(T)}R_{\varepsilon_{P(T)}})}{f_{l_{P(T)}}(\kappa'R_{\varepsilon_{P(T)}})}\right).\quad\text{(A7)}$$

Here, i_l is a modified spherical Bessel function of the first kind, and $f_l(x)$ is one of the Bessel functions.

For $2\nu_{P(T)}R\gg L(L+1)$,

$$g_{PT}(R)\approx\delta_{m_P1/2}\delta_{m_T1/2}\times(-1)^{l_T+1}C^{\rm ex}_{l_P}C^{\rm ex}_{l_T}\sqrt{(2j_P+1)(2j_T+1)}$$
$$\times\left(A_P\frac{\exp(-\nu_PR)}{\nu_PR}+A_T\frac{\exp(-\nu_TR)}{\nu_TR}\right).\quad\text{(A8)}$$

In the derivation of (56) no allowance was made for the contribution from the poles $p=\pm\kappa_{P(T)}$, since the employed wave functions $\psi_{P(T)}$ must be eigenfunctions of the potential $U_{P(T)}$.

If $R\leqslant R_{\varepsilon_P}+R_{\varepsilon_T}$, we obtain the expression (57), where

$$B_{P(T)}=b_{P(T)}[\xi(y_{l_{T(P)}}(\kappa_{P(T)}R_{\varepsilon_{T(P)}}))\xi(y_{l_{P(T)}}\times(\kappa_{P(T)}R_{\varepsilon_{P(T)}}))-\xi(j_{l_{T(P)}}(\kappa_{P(T)}R_{\varepsilon_{T(P)}}))\xi(j_{l_{P(T)}}\times(\kappa_{P(T)}R_{\varepsilon_{P(T)}}))],$$
$$D_{P(T)}=b_{P(T)}[\xi(j_{l_{T(P)}}(\kappa_{P(T)}R_{\varepsilon_{T(P)}}))\xi(y_{l_{P(T)}}\times(\kappa_{P(T)}R_{\varepsilon_{P(T)}}))+\xi(y_{l_{T(P)}}(\kappa_{P(T)}R_{\varepsilon_{T(P)}}))\xi(j_{l_{P(T)}}\times(\kappa_{P(T)}R_{\varepsilon_{P(T)}}))],$$
$$G_{P(T)}=\frac{(-1)^{l_{P(T)}}}{\pi}a_{P(T)}\xi(k_{l_{T(P)}}(\nu_{P(T)}R_{\varepsilon_{T(P)}})),$$
$$b_{P(T)}=\frac{\kappa_{P(T)}(\varepsilon_P+\varepsilon_T-\hbar^2\kappa^2_{P(T)}/m)(\kappa^2_{T(P)}+\nu^2_{T(P)})R^2_{\varepsilon_P}R^2_{\varepsilon_T}}{4(\kappa^2_{P(T)}+\nu^2_{T(P)})(\kappa^2_{T(P)}-\kappa^2_{P(T)})},\quad\text{(A9)}$$

and $I^0_{P(T)}(R,L)$ is the contribution to the matrix element from the pole at the point $p=0$. If $\nu_P=\nu_T$ or $\kappa_P=\kappa_T$, then it is necessary to go to the limit in (56) or (57).

For comparison we also give the expression for $g_{PT}(R)$ obtained under the assumption that only the asymptotic parts of the wave functions contribute to the matrix element:

$$g_{PT}(R)=(-1)^{l_T+m_T+1/2}\frac{\pi}{8}\frac{\hbar^2}{m}C^{\rm ex}_{l_P}C^{\rm ex}_{l_T}\times\sqrt{(2j_P+1)(2j_T+1)}$$
$$\times\sum_L(j_T-1/2,j_P1/2|L0)(j_T-m_T,j_Pm_P|L0)$$
$$\times\left[\left(\frac{\nu_P}{\nu_T}\right)^{l_T}\frac{k_L(\nu_PR)}{\nu_T}+\left(\frac{\nu_T}{\nu_P}\right)^{l_P}\frac{k_L(\nu_TR)}{\nu_P}\right].\quad\text{(A10)}$$

The dependences of the matrix elements $g_{PT}(R)$ on R and the quantum numbers of the single-particle states are given in Ref. 102. Their deviation from the parametrization (38) is shown. Allowance for the shell structure strongly limits the probability of nucleon transfer even if this transition is energetically favored by virtue of the selection rules with respect to the projection of the total angular momentum and spin.

[1] V. V. Volkov, Phys. Rep. **44**, 93 (1978).
[2] R. Bass, *Nuclear Reactions with Heavy Ions* (Springer-Verlag, Berlin, 1980), p. 203.
[3] W. Nörenberg, in *Heavy Ion Collisions*, Vol. 2, edited by R. Bock (North-Holland, Amsterdam, 1980), p. 1.
[4] R. V. Jolos and R. Schmidt, Fiz. Elem. Chastits At. Yadra **12**, 324 (1981) [Sov. J. Part. Nucl. **12**, 129 (1981)].
[5] V. V. Volkov, *Nuclear Reactions of Deep Inelastic Transfers* [in Russian] (Énergoizdat, Moscow, 1982).
[6] W. U. Schröder and J. R. Huizenga, in *Treatise on Heavy-Ion Science*, Vol.

2, edited by D. A. Bromley (Plenum Press, New York, 1984), p. 115.
[7] H. H. Freiesleben and J. V. Kratz, Phys. Rep. **106**, 1 (1984).
[8] R. T. Souza *et al.*, Phys. Rev. C **37**, 1901 (1988).
[9] R. T. Souza *et al.*, Phys. Rev. C **39**, 114 (1989).
[10] R. Planeta *et al.*, Phys. Rev. C **38**, 195 (1988).
[11] A. Türler *et al.*, Phys. Rev. C **46**, 1364 (1992).
[12] R. V. Jolos *et al.*, Yad. Fiz. **50**, 382 (1989) [Sov. J. Nucl. Phys. **50**, 239 (1989)].
[13] W. Bohne *et al.*, Z. Phys. A **313**, 19 (1983).
[14] P. Gippner *et al.*, Z. Phys. A **325**, 335 (1986).
[15] G. Guarino *et al.*, Nucl. Phys. **A424**, 157 (1984).
[16] V. V. Volkov, Izv. Akad. Nauk SSSR, Ser. Fiz. **50**, 1879 (1986).
[17] A. N. Mezentsev *et al.*, in *Fifth Intern. Conf. on Clustering Aspects in Nuclear and Subnuclear Systems* (Kyoto, 1988), Contributed Papers, pp. 214, 216.
[18] K. D. Hildenbrand *et al.*, Phys. Rev. Lett. **39**, 1065 (1977).
[19] T. Tanabe *et al.*, Nucl. Phys. **A342**, 194 (1980).
[20] K. D. Hildenbrand, Nucl. Phys. **A405**, 179 (1983).
[21] A. B. Quint *et al.*, Z. Phys. A **346**, 119 (1993).
[22] N. V. Antonenko *et al.*, Phys. Lett. **319B**, 425 (1993).
[23] S. Agarwal *et al.*, Z. Phys. A **296**, 287 (1980).
[24] A. S. Il'inov, Yu. Ts. Oganesyan, and E. A. Cherepanov, Yad. Fiz. **36**, 118 (1982) [Sov. J. Nucl. Phys. **36**, 69 (1982)].
[25] J. Toke and W. U. Schröder, Ann. Rev. Nucl. Part. Sci. **42**, 401 (1992).
[26] T. C. Awes *et al.*, Phys. Rev. Lett. **52**, 251 (1984).
[27] D. R. Benton *et al.*, Phys. Rev. C **38**, 1207 (1988).
[28] J. Toke, W. U. Schröder, and J. R. Huizenga, Phys. Rev. C **40**, R1577 (1989).
[29] D. Pade *et al.*, Phys. Rev. C **43**, 1288 (1991).
[30] R. Planeta *et al.*, Phys. Rev. C **39**, R1197 (1989).
[31] R. Planeta *et al.*, Phys. Rev. C **41**, 942 (1990).
[32] K. Kwiatkowski *et al.*, Phys. Rev. C **41**, 958 (1990).
[33] J. Toke *et al.*, Phys. Rev. C **44**, 390 (1991).
[34] H. Keller *et al.*, Z. Phys. A **328**, 255 (1987).
[35] G. Beier *et al.*, Z. Phys. A **336**, 217 (1990).
[36] D. H. E. Gross and H. Kalinowski, Phys. Rep. **45**, 175 (1978).
[37] P. Fröbrich, Phys. Rep. **116**, 337 (1984).
[38] W. J. Swiatecki, in *Progress in Particle and Nuclear Physics*, Vol. 4, edited by D. Wilkinson (1980), p. 383.
[39] W. J. Swiatecki, Phys. Scr. **24**, 113 (1981).
[40] D. H. E. Gross *et al.*, Z. Phys. A **299**, 63 (1981).
[41] M. Münchow and W. Scheid, Nucl. Phys. **A468**, 59 (1987).
[42] J. A. Maruhn, W. Greiner, and W. Scheid, in *Heavy Ion Collisions*, Vol. 2, edited by R. Bock (North-Holland, Amsterdam, 1980), p. 397.
[43] R. Schmidt, Fiz. Elem. Chastits At. Yadra **13**, 1203 (1982) [Sov. J. Part. Nucl. **13**, 513 (1982)].
[44] R. Reif and G. Saupe, Fiz. Elem. Chastits At. Yadra **14**, 900 (1983) [Sov. J. Nucl. Phys. **14**, 377 (1983)].
[45] Yu. F. Smirnov and Yu. M. Tchuvil'sky, Phys. Lett. **134B**, 25 (1984).
[46] O. F. Nemets *et al.*, *Nucleon Associations in Nuclei and Nuclear Reactions of Many-Nucleon Transfers* [in Russian] (Naukova Dumka, Kiev, 1988).
[47] A. Lukasiak, W. Cassing, and W. Nörenberg, Nucl. Phys. **A426**, 181 (1984).
[48] D. Berdichevsky *et al.*, Nucl. Phys. **A499**, 609 (1989).
[49] J. Blocki *et al.*, Ann. Phys. (N.Y.) **113**, 330 (1978).
[50] D. H. E. Gross, Nucl. Phys. **A240**, 472 (1975).
[51] N. J. Krappe, Nucl. Phys. **A505**, 417 (1989).
[52] N. V. Antonenko and R. V. Jolos, Z. Phys. A **338**, 423 (1991).
[53] A. Pop *et al.*, Z. Phys. A **329**, 357 (1988).
[54] A. Sandulescu and H. Scutaru, Ann. Phys. (N.Y.) **173**, 277 (1987).
[55] P. N. Isaev, Yad. Fiz. **34**, 717, 914 (1981) [Sov. J. Nucl. Phys. **34**, 399, 510 (1981)].
[56] S. T. Belyaev and V. G. Zelevinskiĭ, Yad. Fiz. **16**, 1195 (1972) [Sov. J. Nucl. Phys. **16**, 657 (1972)].
[57] V. G. Zelevinsky, Nucl. Phys. **A337**, 40 (1980).
[58] V. G. Zelevinskiĭ, in *Proc. of the 12th Winter School of the Leningrad Institute of Nuclear Physics* [in Russian] (Leningrad, 1977), p. 53.
[59] H. J. Fink *et al.*, Z. Phys. A **268**, 321 (1974).
[60] O. Zohni *et al.*, Z. Phys. A **275**, 235 (1975).
[61] W. Nörenberg, Phys. Lett. **53B**, 289 (1974).
[62] L. G. Moretto and J. S. Sventek, Phys. Lett. **58B**, 26 (1975).
[63] S. Ayik, B. Schürmann, and W. Nörenberg, Z. Phys. A **277**, 299 (1976).
[64] S. Ayik, B. Schürmann, and W. Nörenberg, Z. Phys. A **279**, 145 (1976).
[65] H. Hofmann and P. J. Siemens, Nucl. Phys. **A257**, 165 (1976).
[66] H. Hofmann and P. J. Siemens, Nucl. Phys. **A275**, 464 (1977).
[67] D. Agassi, C. M. Ko, and H. A. Weidenmüller, Ann. Phys. (N.Y.) **117**, 140 (1979).
[68] J. Randrup, Nucl. Phys. **A307**, 319 (1978).
[69] J. Randrup, Nucl. Phys. **A327**, 490 (1979).
[70] V. E. Bunakov, Fiz. Elem. Chastits At. Yadra **11**, 1285 (1980) [Sov. J. Part. Nucl. **11**, 507 (1980)].
[71] H. A. Weidenmüller, in *Progress in Particle and Nuclear Physics*, Vol. 3, edited by D. Wilkinson (1980), p. 49.
[72] H. Feldmeier, Rep. Prog. Phys. **50**, 915 (1987).
[73] V. M. Kolomiets, *Local Density Approximation in Atomic and Nuclear Physics* [in Russian] (Naukova Dumka, Kiev, 1990).
[74] V. M. Kolomiets and I. Yu. Tsekhmistrenko, Yad. Fiz. **45**, 1279 (1987) [Sov. J. Nucl. Phys. **45**, 793 (1987)].
[75] P. N. Isaev, Yad. Fiz. **41**, 664 (1984) [Sov. J. Nucl. Phys. **41**, 422 (1984)].
[76] G. G. Adamian, N. V. Antonenko, R. V. Jolos, and A. K. Nasirov, in *Proc. of the Third Intern. School of Nuclear Physics* (Kiev, 1992), p. 342.
[77] G. G. Adamian, N. V. Antonenko, R. V. Jolos, and A. K. Nasirov, Nucl. Phys. **A551**, 321 (1993).
[78] S. Grossman and U. Brosa, Z. Phys. A **319**, 327 (1984).
[79] S. Ayik, Z. Phys. A **292**, 257 (1979).
[80] P. Mädler, Fiz. Elem. Chastits At. Yadra **15**, 418 (1984) [Sov. J. Part. Nucl. **15**, 190 (1984)].
[81] K. T. R. Davies *et al.*, in *Treatise on Heavy-Ion Science*, Vol. 3, edited by D. A. Bromley (Plenum Press, New York, 1984), p. 2.
[82] V. M. Kolomiets, in *Proc. of the 17th Winter School of the Leningrad Institute of Nuclear Physics* [in Russian] (Leningrad, 1981), p. 47.
[83] R. A. Broglia and A. Winther, Nucl. Phys. **A551**, 321 (1972).
[84] R. A. Broglia and A. Winther, Phys. Rep. **4C**, 154 (1972).
[85] V. I. Zagrebaev, Ann. Phys. (N.Y.) **197**, 33 (1990).
[86] K. Dietrich and K. Hara, Nucl. Phys. **A211**, 349 (1973).
[87] G. Bertsch and R. Schaeffer, Nucl. Phys. **A277**, 509 (1977).
[88] J. Bartel and H. Feldmeier, Z. Phys. A **297**, 333 (1980).
[89] S. Pal and N. K. Ganguly, Nucl. Phys. **A370**, 175 (1981).
[90] R. V. Jolos, R. Schmidt, and J. Teichert, Nucl. Phys. **A249**, 139 (1984).
[91] D. Boose and J. Richert, Nucl. Phys. **A433**, 511 (1985).
[92] F. Catara and E. G. Lanza, Nucl. Phys. **A451**, 299 (1986).
[93] M. Baldo *et al.*, Nucl. Phys. **A490**, 471 (1988).
[94] M. Baldo and J. Rapisarda, in *The Response of Nuclei Under Extreme Conditions*, edited by R. A. Broglia (Plenum Press, New York, 1988), p. 201.
[95] S. P. Ivanova and R. V. Jolos, Nucl. Phys. A530, 232 (1991).
[96] R. V. Jolos and A. K. Nasirov, Yad. Fiz. **40**, 721 (1984) [Sov. J. Nucl. Phys. **40**, 463 (1984)].
[97] R. V. Jolos and A. K. Nasirov, Yad. Fiz. **42**, 175 (1985) [Sov. J. Nucl. Phys. **42**, 109 (1985)].
[98] R. V. Jolos, A. I. Muminov, and A. K. Nasirov, Yad. Fiz. **44**, 357 (1986) [Sov. J. Nucl. Phys. **44**, 228 (1986)].
[99] N. V. Antonenko and R. V. Jolos, Yad. Fiz. **50**, 98 (1989) [Sov. J. Nucl. Phys. **50**, 62 (1989)].
[100] N. V. Antonenko and R. V. Jolos, Yad. Fiz. **51**, 690 (1989) [Sov. J. Nucl. Phys. **51**, 438 (1989)].
[101] N. V. Antonenko and R. V. Jolos, Phys. Scr. **32**, 27 (1990).
[102] G. G. Adamyan, R. V. Jolos, and A. K. Nasirov, Yad. Fiz. **55**, 660 (1992) [Sov. J. Nucl. Phys. **55**, 366 (1992)].
[103] G. G. Adamyan, A. K. Nasirov, and V. P. Permyakov, Izv. Ross. Akad. Nauk, Ser. Fiz. **56**, 166 (1992).
[104] R. V. Jolos and A. K. Nasirov, Yad. Fiz. **45**, 1298 (1987) [Sov. J. Nucl. Phys. **45**, 805 (1987)].
[105] G. G. Adamian, R. V. Jolos, and A. K. Nasirov, Z. Phys. A **347**, 203 (1994).
[106] G. G. Adamian, N. V. Antonenko, S. P. Ivanova, R. V. Jolos, and W. Scheid, in *Proc. of the Intern. School-Seminar on Heavy Ion Physics, E7-93-274* [in Russian] (Dubna, 1993), p. 52.
[107] G. G. Adamian, R. V. Jolos, and A. K. Nasirov, in *Proc. of the Intern. School-Seminar on Heavy Ion Physics, E7-93-274* (Dubna, 1993), p. 92.
[108] G. G. Adamian, N. V. Antonenko, R. V. Jolos, S. P. Ivanova, and A. K. Nasirov, in *Intern. Conf. on Nuclear Physics* (Dubna, 1992), p. 217.
[109] R. Vandenbosch *et al.*, Phys. Rev. Lett. **52**, 1964 (1984).
[110] K. Nashinohara and N. Takigawa, Z. Phys. A **324**, 139 (1986).
[111] P. J. Johansen *et al.*, Nucl. Phys. **A288**, 152 (1977).
[112] Z. He, P. Rozmej, and W. Nörenberg, Nucl. Phys. **A473**, 342 (1987).
[113] S. Ayik and W. Nörenberg, Z. Phys. A **309**, 121 (1982).

[114] K. Niita, W. Nörenberg, and S. J. Wang, Z. Phys. A **326**, 69 (1987).
[115] H. S. Köhler, Nucl. Phys. **A343**, 315 (1980).
[116] H. S. Köhler, Nucl. Phys. **A378**, 181 (1982).
[117] R. Schmidt, G. Wolschin, and V. D. Toneev, Nucl. Phys. **A311**, 247 (1978).
[118] J. N. Ginocchio, Phys. Rev. C **8**, 135 (1972).
[119] A. M. Wapstra and G. Audi, Nucl. Phys. **A432**, 1 (1985).
[120] V. M. Strutinskiĭ and V. M. Kolomiets, in *Proc. of the Eighth Winter School of the Leningrad Institute of Nuclear Physics* [in Russian] (Leningrad, 1973), p. 483.
[121] A. N. Mezentsev *et al.*, Izv. Ross. Akad. Nauk, Ser. Fiz. **52**, 2180 (1988).
[122] L. M. Schmieder *et al.*, Phys. Rev. C **37**, 139 (1988).
[123] G. J. Mathews *et al.*, Phys. Rev. C **25**, 300 (1982).
[124] J. Barrete *et al.*, Nucl. Phys. **A299**, 147 (1978).
[125] A. Bohr and B. R. Mottelson, *Nuclear Structure*, Vol. 1 (Benjamin, New York, 1969) [Russ. transl., Mir, Moscow, 1971].
[126] V. A. Chepurnov, Yad. Fiz. **6**, 955 (1967) [Sov. J. Nucl. Phys. **6**, 696 (1968)].
[127] N. V. Antonenko and R. V. Jolos, Z. Phys. A **339**, 453 (1991).
[128] N. V. Antonenko and R. V. Jolos, Z. Phys. A **341**, 459 (1992).
[129] G. A. Adamian, N. V. Antonenko, and R. V. Jolos, Preprint E4-93-324, JINR, Dubna (1993) (submitted to Nucl. Phys. A).
[130] J. P. Bondorf *et al.*, J. Phys. (Paris) **32**, 6 (1971).
[131] N. V. Antonenko, E. A. Cherepanov, A. S. Iljinov, and M. V. Mebel, in *Intern. Conf. on Atomic Masses and Fundamental Constants* (Bernkastel-Kues, 1992), p. 433.
[132] A. S. Iljinov and E. A. Cherepanov, in *Intern. Symposium on Synthesis and Properties of New Elements, D7-80-556* (Dubna, 1980), p. 29.
[133] R. N. Sagaidak *et al.*, Preprint R7-82-890, JINR, Dubna (1982).
[134] J. Wilczynski *et al.*, Phys. Rev. Lett. **45**, 606 (1980).
[135] A. S. Iljinov and E. A. Cherepanov, Preprint R7-84-68, JINR, Dubna (1984).
[136] A. S. Iljinov and E. A. Cherepanov, Preprint R-0064, INR, Moscow (1977).
[137] D. Lee *et al.*, Phys. Rev. C **25**, 285 (1982).
[138] J. Blocki *et al.*, Ann. Phys. (N.Y.) **105**, 427 (1977).
[139] P. Gippner *et al.*, Phys. Lett. **252B**, 198 (1990).
[140] *Handbook of Mathematical Functions*, edited by M. Abramowitz and I. A. Stegun (Dover, New York, 1965) [Russ. transl., Nauka, Moscow, 1979].
[141] B. Jäckel *et al.*, Z. Phys. A **339**, 475 (1991).

Translated by Julian B. Barbour